



**Francisco Lobão
Afonso Teixeira**

**Sensor capacitivo para a monitorização da interface
osso-implante**

**Capacitive sensor for bone-implant interface
monitoring**

**Francisco Lobão
Afonso Teixeira**

**Sensor capacitivo para a monitorização da interface
osso-implante**

**Capacitive sensor for bone-implant interface
monitoring**

Tese apresentada à Universidade de Aveiro para cumprimento dos requisitos necessários à obtenção do grau de Mestre realizada sob a orientação científica do Professor Doutor Marco Paulo Soares dos Santos, Professor Auxiliar Convidado do Departamento de Engenharia Mecânica da Universidade de Aveiro, e Doutor Professor António Manuel de Amaral Monteiro Ramos, do Departamento Engenharia Mecânica da Universidade de Aveiro.

Apoio financeiro dos projetos
UID/EMS/00481/2013-FCT e CENTRO-01-
0145-FEDER-022083

Acknowledgements

A elaboração desta dissertação representa o final do meu percurso académico. Este caminho não teria sido igual (nem melhor) sem os principais intervenientes durante estes 5 anos.

Agradeço ao Professor Doutor Marco Santos, pela disponibilidade, amizade, paciência e apoio prestado durante todo este processo. Obrigado por me ter introduzido à área da inovação e investigação.

Obrigado ao Professor Doutor António Ramos, pela motivação, ajuda e disponibilidade na coorientação deste trabalho.

Um especial agradecimento aos meus pais por me apoiarem incondicionalmente, por me fornecerem o que precisava em qualquer circunstância e por sempre acreditarem nas minhas capacidades. Obrigado por fazerem o bem-estar e a educação dos vossos filhos a vossa principal prioridade.

Agradeço ao meu irmão Bernardo, pelo exemplo a seguir que sempre foi. Pelos conselhos dados durante todos estes anos e ajuda constante.

Um agradecimento a todos os meus amigos do curso e fora dele, por estarem sempre do meu lado nos bons e principalmente nos maus momentos.

Finalmente, um agradecimento especial à Carla, por todos os momentos passados ao longo destes anos e por sempre apoiares as minhas decisões. Fundamentalmente, obrigado por seres quem és.

o júri

presidente

Prof. Doutor Jorge Augusto Fernandes Ferreira

Professor Auxiliar do Departamento de Engenharia Mecânica da Universidade de Aveiro

Prof. Doutor Raul Manuel Pereira Morais dos Santos

Professor Associado com Agregação da Escola de Ciências e Tecnologia da Universidade de Trás-os-Montes e Alto Douro

Doutor Marco Paulo Soares dos Santos

Professor Auxiliar Convidado do Departamento de Engenharia Mecânica da Universidade de Aveiro

palavras-chave

Implantes ativos; Implante instrumentado; Osseointegração; Fixação não-cimentada; Descolamento asético; Monitorização osso-implante; Sensor capacitivo

resumo

Os implantes ósseos usados atualmente não são capazes de substituir integralmente a articulação onde são aplicadas. A redistribuição da carga no osso origina o efeito *stress-shielding*, o que pode provocar perda de massa óssea e migração do implante. O desgaste das componentes integrais do implante também causa alterações na interface osso-implante. Os pacientes com estas complicações, podem ser submetidos a operações de revisão, onde o risco de insucesso e infeções é elevado. Para prevenir tais casos, recentemente foi proposto o conceito de Implante Instrumentado para dotar esta tecnologia com: sistemas de atuação (sobre a interface osso-implante), monitorização da integração osso-implante, sistemas de comunicação implante-exterior e sistemas de geração autónoma de energia. No entanto, uma revisão da literatura mostrou que os sistemas de monitorização propostos não são viáveis para serem incorporados em implantes instrumentados. Este é um estudo preliminar que visa propor um sistema de monitorização capacitivo com configuração em co-superfície listrado integrado num circuito ressonante RLC. Foi desenvolvido um aparato experimental para o teste do sistema *in vitro* usando estruturas de osso porcino. Observaram-se variações de 0,2 fF da capacitância por cada μm de deslocamento relativo entre a estrutura óssea e o sistema de monitorização. Embora preliminar, este estudo apresenta resultados promissores para a monitorização de diferentes interfaces osso-implante usando em sistemas capacitivos em co-superfície.

keywords

Active implant; Instrumented implant; Osseointegration; Cementless fixation; Aseptic movement; Bone-implant monitoring; Capacitive sensor

abstract

The prostheses currently used, are not able to fully replace the joint where they are applied. The redistribution of the load in the bone causes stress-shielding, which origins loss of bone mass, and migration of the implant. Also, the wear of the integral components of the prosthesis causes changes between the interface of the bone and the implant. Patients with these complications can be submitted to review surgeries, where the risk of failure and infection is high. To prevent such cases, instrumented prosthesis have been recently proposed, to enhance this technology with: actuation systems (over the bone-implant interface), osseointegration monitoring, communication systems between implant-exterior and systems capable of generating energy autonomously. However, a review over these technologies showed that the proposed monitoring systems are not feasible to be incorporated into instrumented implants. This is a preliminary study which aims to advocate a monitoring capacitive system with a cosurface stripe pattern integrated in a RLC resonant circuit. An experimental apparatus was developed to test the system *in vitro* using a porcine bone. Variations of 0,2 fF in the capacitance were observed, for each μm of relative movement between the bone and the monitoring system. Although preliminary, this study presents promising result for monitoring different bone-implant interfaces using a cosurface capacitive system.

Table of Contents

1. Introduction.....	1
1.1. Scope.....	1
1.2. Goals	2
2. Literature Review.....	3
2.1. Pathologies.....	3
2.2. Need of arthroplasty.....	4
2.3. Implant Failures.....	7
2.4. Aseptic Loosening.....	9
2.5. Osseointegration monitoring systems	12
2.5.1. Previous reviews.	12
2.5.2. Imaging Techniques	12
2.5.3. Vibration.....	15
2.5.4. Acoustic Emission.....	19
2.5.5. Magnetic Induction	21
2.5.6. Electric Impedance.....	22
2.5.7. Micromotion.....	23
2.5.8. Strain	24
2.5.9. Other Identification Methods	24
2.6. Comparison among osseointegration sensors.....	25
3. Methods	28
3.1. Detection method	28
3.2. RLC circuit development	31
3.2.1. Electric components selection and capacitance review	31
3.3. Printed circuit board preparation.....	33
3.4. Experimental apparatus	34
3.5. Experimental procedure	39
4. Results.....	41
4.1. Capacitance variations without saline solution.	41
4.1.1. By measuring the resonant frequency	41
4.1.2. By measuring phase shift	44
4.2. Capacitance variations with saline solution	47
4.2.1. By measuring the resonant frequency	47
4.2.2. By measuring phase shift	50
5. Discussion.....	52
6. Conclusions and future work	53
7. Bibliography	54

Figures

Figure 1: (a) Cosurface-based stimulators according to a striped pattern. (b) Example of instrumented hip prosthesis with these stimulators [11]	2
Figure 2: Diagnosis for hip arthroplasty in USA (2012-2015) [13].....	4
Figure 3: Age distribution of knee arthroplasty procedure in the USA,2012- 2015 (N=169 060) [13]	5
Figure 4: Percentage of revision surgery for hip and knee arthroplasty between 2012 and 2015 in the USA [13]	7
Figure 5: Percent of all hip revisions according to the diagnosis in the USA [5]. “all other codes” portion refers to ICD code 992 for unclassified complications [38]......	9
Figure 6: Bone turnover schematic [44].....	10
Figure 7: The effect of stress shielding on a hip stem. Left: Fixed prosthesis. Right: Loosened prosthesis [56]	11
Figure 8: Stem/cement radiolucency [70].	13
Figure 9: Stem/cement radiolucency with Arthrography [71]	13
Figure 10: Equipment used for vibration measuring [82]	16
Figure 11: System concept of an embedded accelerometer [91].....	18
Figure 12: Ultrasonic transducer operation schematic [97]	20
Figure 13: Magnetic induction system [109]	22
Figure 14: Schematic of the measuring system. The electrode induces electrical impedance [106]	23
Figure 15: Schematic of the capacitive sensor for interface monitoring. 1. Bone portion; 2. Dielectric (The dielectric includes the area/volume above the electrodes (3)); 3. Electrodes	28
Figure 16: Example of a voltage ratio as a function of frequency in a RLC circuit (L=10 mH, C=10 pF, R=1 kΩ). A resonant frequency is about 500 kHz.....	29
Figure 17: Phase shift in a RLC series circuit.....	31
Figure 18: Capacitance of wet bovine bone as function of frequency in axial, radial and circumferential directions [130].....	32
Figure 19: Schematic of the PCB design (image taken from Eagle 8.1.0 free version). L –10 mH inductance; R – 1 kΩ resistor;.....	33
Figure 20: Produced PCB.....	33
Figure 21 Finished PCB with welded electric components	34
Figure 22: Multi-test machine	35
Figure 23: Final assembly of the experimental apparatus	36
Figure 24: Part (2) of the experiment structure	37
Figure 25: Part (3) of the experiment structure	38
Figure 26: Part (4) of the experiment apparatus.....	38
Figure 27: Equipment used for generating the input signals and measure the output signals. Left: Signal Generator, Right: Oscilloscope.	39
Figure 28: Measurement setup.	40
Figure 29: Bone portion measured	40
Figure 30: Results measured through resonant frequency measurement, for a bone free of serum.	42
Figure 31: Adjusted results between 0 and 200 μm, for measured resonant frequency in a free of serum bone	43
Figure 32: Results measured through phase shifts, for a bone free of serum.....	45
Figure 33: Adjusted results between 0 and 200 μm, for measured through phase shift, in a free of serum bone	46
Figure 34: Results measured through resonant frequency measurement, for a bone previously embedded with saline solution	47
Figure 35: Results measured through resonant frequency measurement, for a bone previously embedded with saline solution with $\Delta y=50 \mu\text{m}$	48

Figure 36: Adjusted results between 0 and 200 μm , through resonant frequency measurement, for a bone previously embedded in saline solution.....	49
Figure 37: Results measured through phase shifts, for a bone previously embedded in saline solution.....	50
Figure 38: Adjusted results between 0 and 200 μm , through phase shift measurement, for a bone previously embedded in saline solution	51

Tables

Table 1: Revision rate of total hip arthroplasty.....	6
Table 2: Revision rates of total knee arthroplasty.....	6
Table 3: Revision rates of total shoulder arthroplasty.....	6
Table 4: Comparison of instrumented loosening monitoring systems.....	27
Table 5: Quadratic tendency line equations for $\Delta y=50 \mu\text{m}$ and $\Delta y=100 \mu\text{m}$, through resonant frequency measurements, for a bone free of serum.....	42
Table 6: Tendency linear line equation for the measured results, for resonant frequency measurement, in a bone free of serum.....	44
Table 7: Quadratic tendency line equation for the measured results, through phase shifts, for a bone free of serum.....	45
Table 8: Linear tendency line equation for the measured results, through phase shifts, for a bone free of serum.....	46
Table 9: Quadratic tendency line equation for the measured results, through resonant frequency measurement, for a bone previously embedded with saline solution.....	48
Table 10: Linear tendency line equation for the measured results, through phase shifts, for a bone previously embedded saline solution.....	49
Table 11: Quadratic tendency line equation for the measured results, through phase shift measurement, for a bone previously embedded with saline solution.....	50
Table 12: Linear tendency line equation for the measured results, through phase shifts, for a bone previously embedded saline solution.....	51
Table 13: Global results for the experimental procedure.....	52

1. Introduction

1.1. Scope

Total joint arthroplasty (TJA) is currently a typical procedure for treating pathologies associated with the degeneration of synovial joints, such as rheumatoid arthritis, osteoarthritis, or rupture joints. Other procedures can be used to remove or alleviate pain and discomfort on the patient such as arthrodesis, physiotherapy, and pharmaceutical medication. However, only joint arthroplasty restores fully or partially the articulation motion. This procedure can also be used to cure patients with a history of “weak joint”, with several fractures or dislocations [1], [2] .

Millions of TJA are performed each year. Most joint replacement procedures have a success rate higher than 80%, especially for hip and knee arthroplasties [3]. The prosthesis applied are divided into two distinct ways of fixation: cemented and cementless (press-fit) fixation. With the use of cement, the initial stability of the implant is in most cases superior, however, concern arise when analysing long-term fixation. The degeneration of the bone cement can cause a premature loosening of the implant and/or particle induced osteolysis. Therefore, cementless fixation is proven to be a more appropriate procedure for long-term fixation [4]. Thus, a further focus is given to cementless fixation in this work. After one year of surgery, the predominant reasons for press-fitted implemented prosthesis to failure, are infections-related and/or lack of initial bone-implant integration [4], [5]. The occurrence of infection can be associated with many susceptible variables such as the: operation room, time of surgery, the use of antibiotics and several other problems associated with the patient. In many cases of infection, the cause is not revealed [6], [7]. Patients which TJA is successfully carried can live a normal life for over than 20 years. However, complications may arise for patients with a long-term prosthesis. Today the most frequent cause of revision procedures for patients with a long-term prosthesis is aseptic loosening. This happens due to wear of the components and of the surrounding human tissue, stress shielding, and bone resorption. This type of procedures depicts a higher risk and uncertainty. The success rate drops substantially when compared to primary arthroplasty [8]–[10].

In order to prevent unnecessary revision procedures, micro gaps between the implant and the bone must be spotted before critical loosening occurs. Current loosening detection methods are unable to detect small interface detachment between the prosthesis and the bone (as show in section 2.7). The imaging techniques used, such as X-ray and arthrography, lack the resolution needed to identify small-scale loosening states. In this manner, instrumentation of passive implants with sensors can hold potential for identification of loosening states before critical conditions occur.

Several methods were proposed through the years, however, none of them fully achieves all the conditions that a reliable detection system must retain.

1.2. Goals

In this dissertation, a new monitoring method is proposed and tested. The main goal was to analyse the potentiality of a co-surface capacitive system to operate in bone-implant monitoring. The concept is based on capacitance variation that occurs following bone-implant interface changes. The method is established on the notion that when the bone detaches from the prosthesis, the biophysical conditions between the bone and prosthesis alter. These variations can be measured using a monitoring system with ability to simultaneously stimulate the dielectric and capture resonant frequency variations. The solution presented is a set of identical stripe-shaped electrodes separated with equal gaps. This concept can be observed in Figure 1.

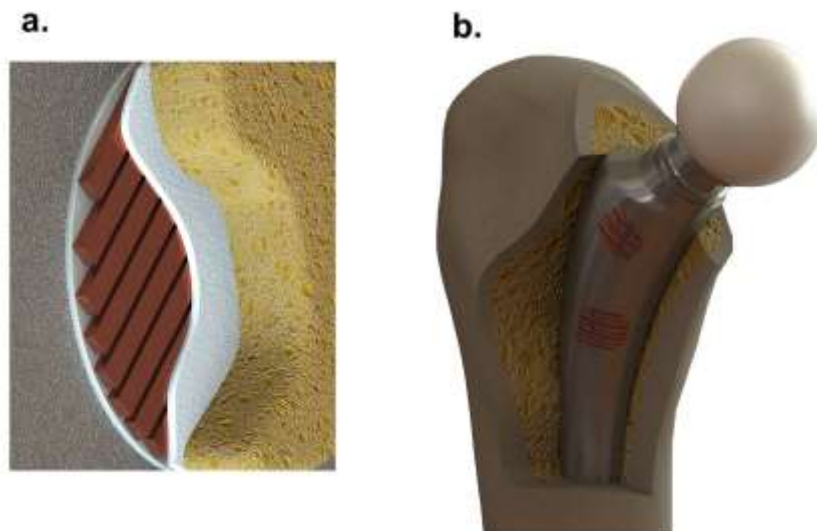


Figure 1: (a) Cosurface-based stimulators according to a striped pattern. (b) Example of instrumented hip prosthesis with these stimulators [11]

To demonstrate that this concept hold potential for the implementation of suitable monitoring systems, a test bench, capable of producing distinct contact conditions, was designed and developed. The testing system was projected to simulate an actual joint interfacing a monitoring system. Then,

a resonant RLC electric circuit was designed and constructed in a printed circuit board (PCB). Resonant frequency measurements were conducted with different interface conditions, which allow to infer capacitance variations for different interface conditions. The results obtained allow to envisage the feasibility of this methodology. Therefore, this work represents the starting point for the development of an innovative and reliable monitoring system for instrumented prosthetics.

2. Literature Review

2.1. Pathologies

Several diseases weaken the bones and joints, generating pain, swelling and consequently motion inability. Rheumatoid arthritis, osteoarthritis, and polyarthritis are examples of such diseases.

Rheumatoid arthritis is an inflammatory autoimmune disease, associated with the premature destruction of the cartilage and articular structures in synovial joints, resulting in bone erosion, which can lead to deformity if not treated [12]–[15]. The dysfunctional autoimmune system and inflammatory response causes the degeneration of the joint [12]. It is characterized by joint pain, stiffness, swelling, and loss of range motion of the affected joint [12]–[14]. The incidence of rheumatoid arthritis in the adult population is between 0.5% and 1% [13]. Although the pathogenic has been generally perceived, the cause of rheumatoid arthritis remains unknown [14]. It is noteworthy the decrease rate of patients diagnosed with rheumatoid arthritis which are admitted for joint replacement [10], [16]. This is due to the fact that newer and safer medical therapies and procedures prevail in the treatment of this disease. Osteoarthritis is the most incident type of arthritis [10], [17]. Osteoarthritis is described as a degenerative disease, characterized by progressive mechanical stress to the joint, in combination with biochemical alterations of the cartilage [17], [18]. Disruption of the joint causes pain, joint swelling, and decrease of range motion. Osteoarthritis is more common in the hand, knee and hip joints, and is the most common reason for total hip and knee replacement [17]. It is evident that the prevalence of osteoarthritis increases with the age group, although it is being observed increasing incidences in young (less and 65 years old) and/or active patients [13], [19]. The incidence of these diseases is strongly associated with environmental and genetic factors. Occurrence rates according to the sex type of the patient are also distinct [13], [17], [19]. For example, before 50 years of age, osteoarthritis is more common in men. However, after the age of 50, women are more affected by hand, foot and knee osteoarthritis [17]. Avascular necrosis is also one of the most predominant diseases affecting patients that are admitted for TJA. This disease, also commonly named osteonecrosis, is the destruction of bone tissue due to poor blood supply.

Avascular necrosis often occurs in the femoral head. The accumulated stress fractures in the trabeculae area, which are not repaired, collapses and dislocates the femoral head, which, consequently, impose low blood irrigation and, finally, necrosis of the bone occurs. The progression of this disease results in the necessity of total hip replacement [20], [21]. Concerning the impact that each disease has, it is easy to understand by observing Figure 2, the influence that osteoarthritis has on the proliferation of total hip arthroplasty. The same occurs for knee, shoulder and most joints [10], [16], [22], [23].

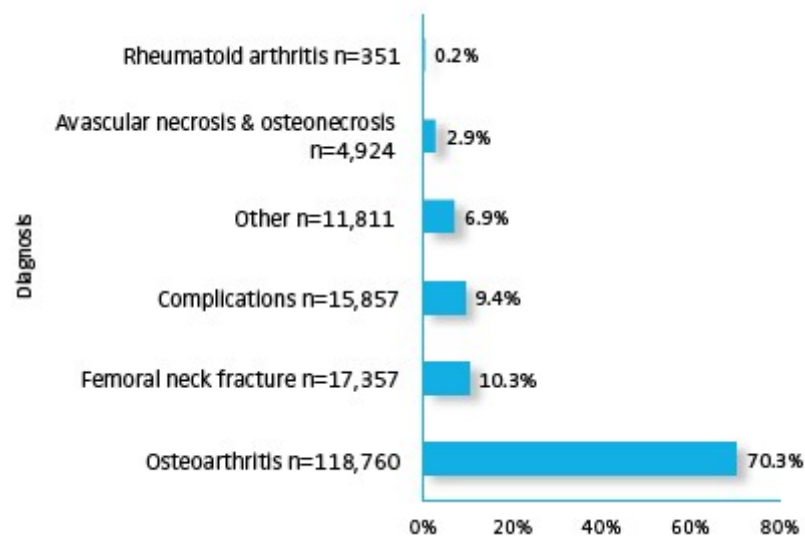


Figure 2: Diagnosis for hip arthroplasty in USA (2012-2015) [13]

2.2. Need of arthroplasty

At the present time, total joint arthroplasty is a standard procedure to treat degenerative and rheumatologic diseases, especially in knee and hip joints [3], [24], [25]. For instance, nowadays over one and a half million total knee replacements are performed every year [3]. The amount of total joint surgery performed increases each year and has been projected to rise in the subsequent years as the longevity of the human population also grows [2], [25], [26]. A demand of 572,000 total hip arthroplasties and 3,48 million total knee arthroplasties has been estimated to take place by 2030 in the US [2]. More than 1 million total hip arthroplasties are performed worldwide every year [27]. Based on demographic change, hip replacement is projected to increase around 15% in 2026 also in the US [28]. However, incidences are country-related and estimations based on demography are difficult to obtain. For instance, although the population of New Zealand grew 17% between 1999-2015, ankle arthroplasty doubled [29], [30]. The number of shoulder arthroplasties performed has also increased in the last years. Between 1993 and 2008 shoulder arthroplasty grew 167% in the

United States [31]. By observing and estimating through the increase levels of shoulder total arthroplasty in 2007, one can observe the augmentation of this medical procedure is between 192% and 322% in the current year, since 2007 [32]. Furthermore, TJA has been reported to expand to patients under 65 years [25]. Medical devices implanted on more active or young patients, are more likely to fail and be admitted to revision operations [33]. The incidence of TJA surgery on younger generations demands an optimization of current prevention methods and prosthesis. The growth of TJA compels the number of revision procedures to raise as well. TJA revision is a more challenging and expensive procedure, when compared to primary joint arthroplasty, as a result of more blood loss and bone loss involved, as well as longer operation time required [9], [34]. Furthermore, additional complications are more susceptible to arise intraoperatively and postoperatively, such as infections, ligamentous instability, several comorbidities and, in the extreme case, death [6], [8], [9], [34]–[36]. The mean age for primary knee arthroplasty and revision is represented in Figure 3. For instances, according to the registries by the “Australian Orthopaedic Association”, patients with an age lower than 55 years, represent 14,3% of the total hip and 7% of total knee replacement performed in the last 15 years [22]. Knee replacement is performed in a mean age of 66,8 years while revision procedure is of 61,8 years [10].

Although the success rate of joint arthroplasties is generally between 90% and 100% within a 10-year period after implant insertion, especially for knee and hip replacement, the number of patients admitted to revision surgeries is still significant. The amount of revision surgeries performed can be perceived by observing Tables 1,2 and 3, which represent the surgery rates obtained through registries from four different countries, namely Portugal, US, UK and Norway.

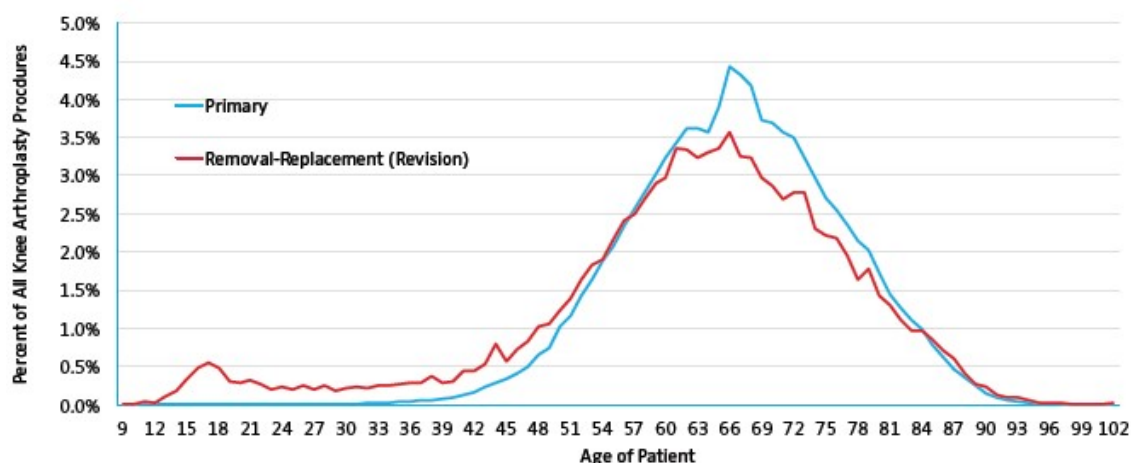


Figure 3: Age distribution of knee arthroplasty procedure in the USA,2012- 2015 (N=169 060) [13]

Country	Period	Primary replacements	Revision replacements	Revision Percentage
Portugal [37]	2015	3 446	420	12,2 %
USA [10]	2012-2015	169 060	17 180	10,2 %
UK [16]	2015	89 288	7 621	8,54 %
Norway [23]	2015	8 402	1 392	14,2 %

Table 1: Revision rate of total hip arthroplasty

Country	Period	Primary replacements	Revision replacements	Revision Percentage
Portugal [37]	2015	3 253	221	6,79 %
USA [10]	2012-2015	258 121	22 403	8,68 %
UK [16]	2015	98 591	6 104	6,19 %
Norway [23]	2015	6 093	554	8.3 %

Table 2: Revision rates of total knee arthroplasty

Country	Period	Primary replacements	Revision replacements	Revision Percentage
Portugal [37]	2015	201	24	11,94 %
USA [38]*	2005 to 2013	6 336	360	5,60 %
UK [16]	2015	5 465	705	12,90 %
Norway [23]	2015	642	58	8,30 %

Table 3: Revision rates of total shoulder arthroplasty

*Sum of registries from 2 of 6 regions from Southern California and Northern California (with 7 million members)

As previously mentioned, the amount of revision procedures reported over the last few years is estimated to increase in the next few years. The burden of revision procedures can be observed through Figure 4.

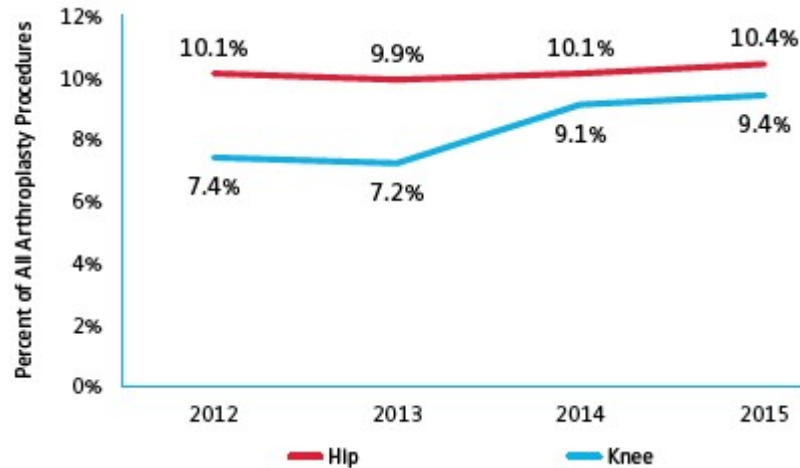


Figure 4: Percentage of revision surgery for hip and knee arthroplasty between 2012 and 2015 in the USA [13]

As the rates of TJA increase, the optimization of current monitor and prevention methods must be carried out. To improve current implants, failures associated with them, are in the next chapter assessed.

2.3. Implant Failures

The success of an implanted medical device is contingent to several different variables. Before mentioning them, is important to understand the factors that influence the implant performance. The main features to have in consideration when designing implants are:

(a) The *geometry* of every element intrinsic to the device, as well as the interaction between each component, and associated kinematics. It is fundamental to understand the mechanical interaction between each element of the implants and the surrounding system.

(b) The *type of material* used for the implant. Consideration for the stress, strain and fatigue resistance properties of the prosthesis are important to prevent malfunctions. Also, good biocompatibility, favourable chemical properties and bioactivity are essential. Accidents, such as precipitate corrosion or wear of the components, may cause infections and prevent long term reliable usage of the implants.

(c) *Range of motion* permitted. The fundamental advantage of performing an arthroplasty is the preservation of the joint motion. The mobility of the prosthesis implanted, should at least ensure the fundamental biomechanical movements. For example, suitable knee joint implants should, perform sufficient flexion and extension angles degrees that allow patients to perform normal daily activities. Researchers have also found that implants with mobile components are less stressed than fixed elements [39].

(d) *Fixation* method. The implant fixation is critical for long-term success. Developers must reflect on cemented, cementless or hybrid fixation (the last composed by cemented and uncemented components) [4]. Bone cement application reduces post operation pain and increases the initial stability of the implant system [5]. Using a cementless application, initial stability is harder to achieve because suitable mechanical biological interplay is required. Considering that arthroplasties are mainly performed in older patients, who usually present poor bone quality, surgeons tend to use cement. The disadvantage of this method is related to long-term degradation of bone cements [4].

(e) *Medical procedure*. Misalignment and infections are examples of problems associated with poorly executed surgery procedures. Every procedure indication as well as instrumentation, should be provided. To decrease complications during and after operation, surgeries must be simple and the insertion method must be clearly described.

(f) *Revision surgery*. If, for any reason, the implant fails, a revision procedure is inevitable. Prosthesis must be designed keeping in mind the removal procedure.

Concluding, it is fundamental to understand and predict the possible collapses of current bone implants systems in order to design the new generations of implant technologies. The causes of implant failures are mainly: mechanical, chemical and/or biological (as result of the human body response) [39]. The material of the implant affects the outcome of implants. These may wear, fracture or deform because of the loads and stress they are undergone, that is why materials play a vital role on the (long-term) success of the implant. The main causes for implants to early fail are aseptic loosening, instability/dislocation and infection [7], [10]. Dislocation can occur when implants are not adequately positioned or loosed. If it is misaligned, the risk of micromotion increases. Osseointegration won't occur in a proper way in unstable implants. Figure 5 represents the percentage of hip revisions for each complication in the USA.

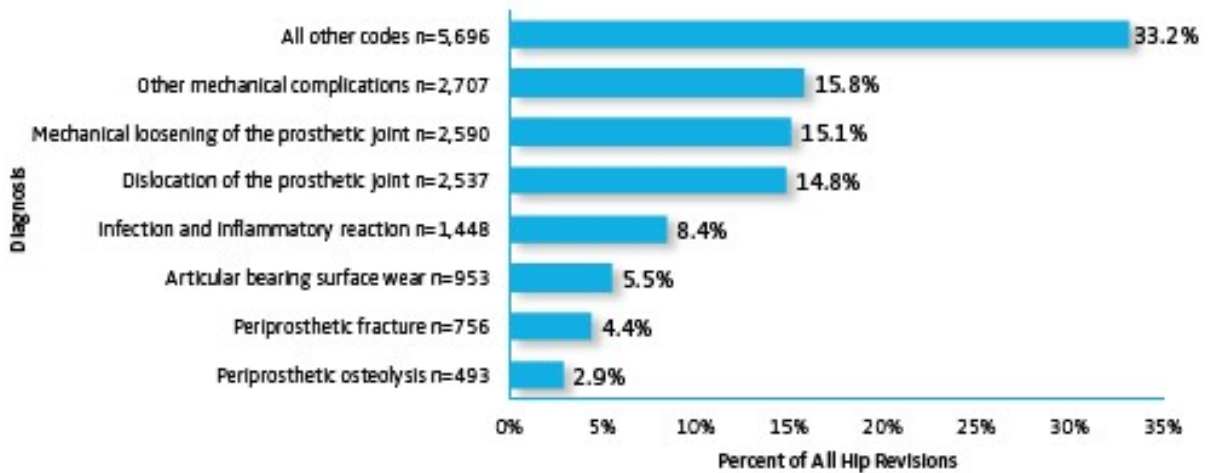


Figure 5: Percent of all hip revisions according to the diagnosis in the USA [5]. “all other codes” portion refers to ICD code 992 for unclassified complications [38].

Fixation failure between the stem and the bone is one of the main reasons for long term prosthesis failure and, thus, revision operations [1], [27], [40]–[42]. In the next chapter, a detailed description of the mechanisms that originate aseptic loosening are defined.

2.4. Aseptic Loosening

Aseptic loosening occurs when the implant loosens with respect to the bone due to any cause other than infection. To fully understand the loosening mechanisms, it is fundamental to first comprehend the bone adaptation to mechanical loadings, as well as its capability of remodelling. The average adult replaces approximately 10% of its bone matrix every year [43]. Bone renovation restores micro fissures caused by mechanical loadings, while maintaining the appropriate calcium levels. This process is executed by two distinct cells: osteoblasts, responsible for generating new bone, and osteoclasts that breaks down bone tissue and resorbs it. Figure 6 represents the remodelling schematic, along with the different time phases of bone replacement [44]. It begins with the osteoclast activity (phases I, II), osteoblastic activity (phase III) and then the mineralization stages (phases IV and V).

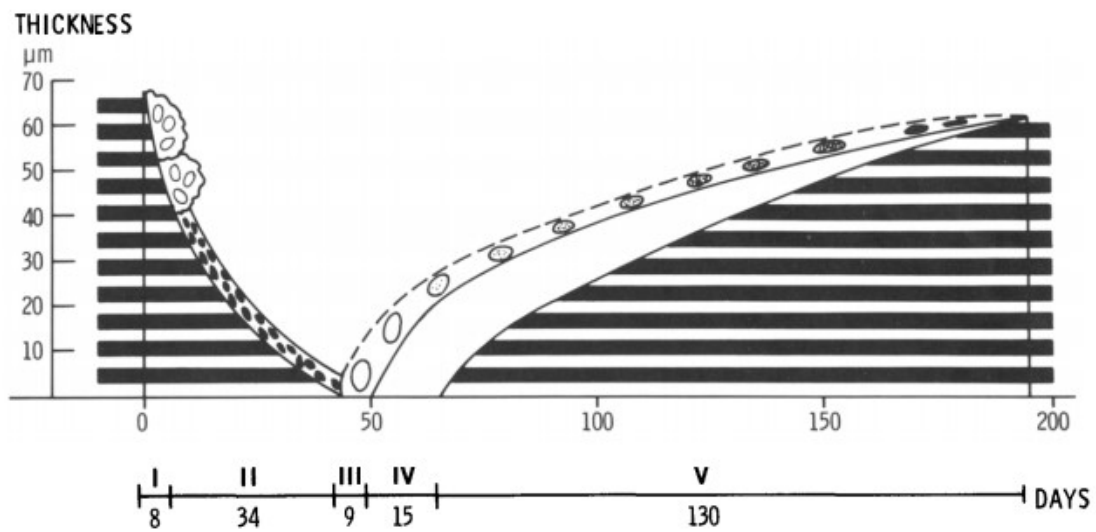


Figure 6: Bone turnover schematic [44]

The bone is submitted to several stresses throughout the life time of a human being. To prevent fractures, the bone can adapt to the physical activity offered. For instances, a football player or a professional marathon has more minerals in the leg bones than a normal individual. Similarly, a person with more body weight has also a higher bone density [45]. On the other hand, when bone is not sufficiently stimulated by mechanical loading, its mass decreases. In this last event, osteoclast activity or osteolysis is predominant.

Premature osteolysis is a serious problem that limits the long-term success of current implants and causes aseptic loosening between the bone and implant. Although loosening is the most frequent cause of revision operations, causes for such event are not entirely understood. Aseptic loosening has a multifactorial diagnosis, which led investigators to formulate multiple cause theories. Carlsson et al. [46], concluded, by analysing 70 total hip arthroplasties, that bone resorption occurs as a result of mechanical stress and has no relation with infection. Also, osteolysis may be equally distributed around the implant or in specific locations, creating islands of bone deficiency. Schmalzried et al. [47] considered that aseptic loosening is strictly related to wear particles. Studying tissue from 34 hips, the authors found that bone resorption occurred when the tissue studied contained polyethylene (PE) debris. They detached into the joint fluid, activating macrophages and therefore triggering osteoclasts and bone resorption. Doorn et al. [48] investigated loosening on metal-metal hip prosthesis. They stated that aseptic loosening still happened, however the activity from the macrophages in storing the wear particles was less than the one observed for polyethylene debris. This is because of the small size of the metal particles. One can conclude that metal particles are also related to aseptic loosening.

It is important to mention the role that cement plays in both fixation and later debonding. Cement is generally used to improve fixation of the interface between bone and prosthesis. It is very commonly used, especially in elderly patients as a result of poor bone quality [49]. According to the mechanical stress actuating between the implant and the cement, debris can have different size and distribution. Similarly to metal or PE, cement debris play a major role in aseptic loosening. One other aspect to consider is the possibility of cement fracture. The chance of a cement to fracture is related to the porosity of the material used. It is common sense to reduce the porosity as much as possible [50].

Many authors concluded that PE together with cement debris are among the main causes for aseptic loosening to arise [47], [49], [51], [52]. Regarding ceramic prosthesis, Warashina et al. [52] proved, through animal studies, that less bone resorption as well as inflammatory response arises due to resultant debris. It has been proven that ceramic debris activate macrophages if they have relatively large volume ($>100 \mu\text{m}^3$). However, Hatton et al. [53] argue that, given the volume necessary to activate osteolysis and the low wear rates even with critical loosen states, it is improbable that ceramic debris activates macrophages.

Replacing a joint by inserting an implant, remodels the bone loading conditions [49], [54], [55]. This means that some portions of the bone may be load free while others might be submitted to excessive load magnitudes. This leads to bone loss on those portions of bone that are not mechanically (and, then, electromagnetically) stimulated. This phenomenon is commonly named stress shielding. It is based on Wolff J. theory for the bone behaviour when submitted to loading. As this author stated, bone responds to the series of loads, adapting its geometry and density accordingly. If loads applied decreases, so does the bone density. Figure 7 shows the effect of stress shielding in a hip prosthesis. The arrow points out the zone that is unstressed and consequently, bone tissue that was lost.



Figure 7: The effect of stress shielding on a hip stem. Left: Fixed prosthesis. Right: Loosened prosthesis [56]

Independently of the origin and reason for loosening, suitable monitoring methods must be developed, so that revision procedures can be prevented.

2.5. Osseointegration monitoring systems

This section efforts on identify and analyse the osseointegration monitoring concepts proposed through the years. The way this review is organized is now described. Initially, previous reviews are outlined, and the limits of them are assessed. Afterwards a description of current monitoring systems is performed. The need for an optimized monitoring system are then defined. A general description of each instrumented implant follows, as well as an evaluation of the advantages and limitations of each approach. At the end, a comparison, based on the requirements formerly presented for each methodology is assembled.

2.5.1. Previous reviews.

Some former evaluations of existing methods have been made in previous year. Varga M. and Wolter [56] analysed existing sensors and imaging technics that identified loosening in hip implants. Yet, very few focus is given to the existing monitoring systems and it does not cover the whole spectrum of existing devices. Ruther *et al.*[57] also assessed proposed systems to detect loosening on total hip replacement prostheses. However, they only review vibration based methods and don't detail their analyses. Andreu-Perez J. *et al.* [58] also perform a review on a large variety of sensors, yet very few focus is given to smart implants capable of monitoring loosening states. Lastly two reviews [59]–[61] focused on monitoring osseointegration in dental implants. They cover a wide range of imaging and sensor systems for implant stability.

2.5.2. Imaging Techniques

Numerous methods are used to monitor osseointegration. The main traditional clinical procedure is the use of X-rays. Zhang *et al.* [62] studied the reliability of the use of X-rays to detect loosening through the use of radiolucencies. He concluded that only 0,7 mm radiolucency's thickness are marginally reliable. Thus, X-rays are incapable of detecting, properly, information about the bone-implant interface. An X-ray of a stem/cement interface is showed in Figure 8, with the respective visible thickness.

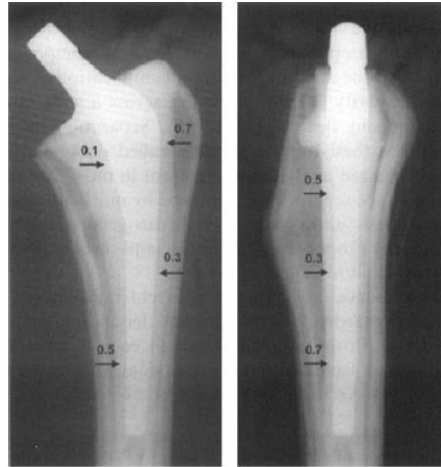


Figure 8: Stem/cement radiolucency [70].

One other method is the use of arthrography. The injection of a dye like material can create a contrast in the captured X-rays and, consequently, enhance the sensitivity of the procedure, capturing smaller radiolucencies, which would not be picked up using plain radiographs, as presented in Figure 9. [63]. Although providing a higher resolution, it is more invasive, which translates into more risk associated. Arthrography is still very limited in providing a correct assessment of the bone-implant integration, as Mulcahy D. *et al.* [64] concluded in his work. Nonetheless, recent published studies revealed good results in using radionuclide arthrography [65]–[67]. For instances in French *et al.*[65] study, a sensitivity of 93% and a specificity of 83% was found in 27 patients.

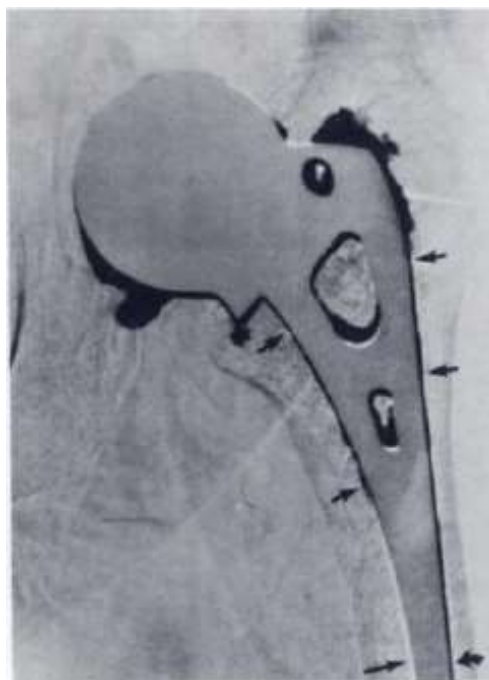


Figure 9: Stem/cement radiolucency with Arthrography [71]

In addition to these techniques, scintigraphy is also a procedure used to monitor osseointegration. It consists in the injection of radioactive metals, which concentrate in areas of newly formed bone tissue. Since a loose prosthesis is characterized by increased osteoclastic activity around it, a bone scan can show osseointegration. However, it may also detect osteoblastic activity associated with bone infection, and there is no method to differentiate both phenomenon [68]. Also, a major concern using this method is the risk of infection connected to the intraarticular injection [69].

The limitations of traditional approaches, compel many authors to find a feasible and accurate method to oversee osseointegration after arthroplasty. The most promising path, is the instrumentation of current non-instrumented passive implants. Several instrumented designs were proposed through the years, not only to detect aseptic loosening, but also different biomechanical and thermodynamic data relevant for the design and material optimization, as well as for rehabilitation purposes. As Santos *et al.* [70] stated, instrument implants must be able to: “(a) monitor their own state and the physiological states of the tissue surrounding the implants; (b) perform therapeutic actuations in order to prevent failures; (c) communicate with the external systems, namely with medical staff”. Instrumented implants began in the 60s with the design proposed by Rydell [71]. Rydell performed an *in vivo* investigation of two patients over different activities. With internal strain gauges in the neck flange of a hip prosthesis, he was able to determine the magnitude of the forces acting on the hip joint, as well as their direction. The data was transferred by percutaneous connections to an external data acquisition system. Since then, similar instrumented implants were implemented to collect information about the loading dynamics and temperature, which theoretical methods could not predict with certainty. In recent years, some authors proposed different instrumented implants to predict aseptic loosening. However, to date, all proposed technologies have undesirable complications or limitations on the conceived concepts. Every system used is generally described as follows: a component, internal or external, excites electrically, magnetically or mechanically an element inherent to the implants; this reaction, then, alters some initial characteristic of the system which is then measured. It is of note that, to this date only instrumented passive implants have been fully designed and implanted in human beings [70]. In this chapter, a description of current procedures is made, as well as an evaluation of the feasibility of each approach. There are some requirements that an osseointegration monitoring system must fulfil. A viable monitoring system must be able to operate without interfering in the fixation process after the prosthesis is implanted, so that osseointegration is accomplished. The sensor mechanism must be able to integrate within the implant. Also, it needs to be of flexible application, in order to be applicable in different prosthesis with variable structure and geometry. The monitoring system must

be controllable so that various regions of the tissue can be monitored while functioning as a therapeutic actuator. Finally, it is essential for the system to be able to detect fixation failures before severe loosening occurs. The described past methods will be reviewed based on these mentioned requirements.

2.5.3. Vibration

The most intensively used and studied method is based on vibration analysis. It was first applied to monitor loosening after a total hip replacement. It consisted in transferring a known vibration frequency, using a shaker or a similar apparatus, and then recording the output waveform near the hip and the implant, or inside the implant. Sonstegard *et al.* [72] were the first to suggest the diagnosis of loosening prosthetic by measuring alterations in the natural resonant frequency of the bone-implant. Van der Perre and Lowet [73] also reported that when loosening occurred there was a decrease in the resonant frequency. Rosenstein *et al.* [74] performed the first *in vitro* examination of this technique, by applying a known vibration and then capturing acceleration variations using an accelerometer. The system is represented in Figure 10.

A pilot clinical study was performed, using this procedure, to seven patients, who were admitted for revision surgery due to aseptic loosening. Both the shaker and the sensors were not inherent to the prosthesis. In both trials, the frequency was analysed and revealed multiple harmonics associated with loosened prosthetics. It is relevant to mention that the performed clinical study did not perceive early loosening or micro loosening, considering that the patients evaluated were already indicated to have a revision operation due to poor bio-integration of the prosthesis. Meredith *et al.* [75] performed an *in vivo* investigation on the resonance frequency of titanium implants inserted on rabbits' tibia. This was accomplished by positioning a transducer, constituted by two piezo-ceramic elements, onto an external abutment of the implant. One of the piezoelectric element functioned as an actuator and the other as a sensor. Measurements were made in a time span of 168 days. It was possible to identify resonance changes according to the fixation degree of the implant. However, this work aimed to solely prove that resonance can be used to predict loosening. The system projected can't be translated for instrumented implants since a large portion of the monitoring device is prominent from the prosthesis. This consequently limits the prosthesis flexibility and osseointegration.

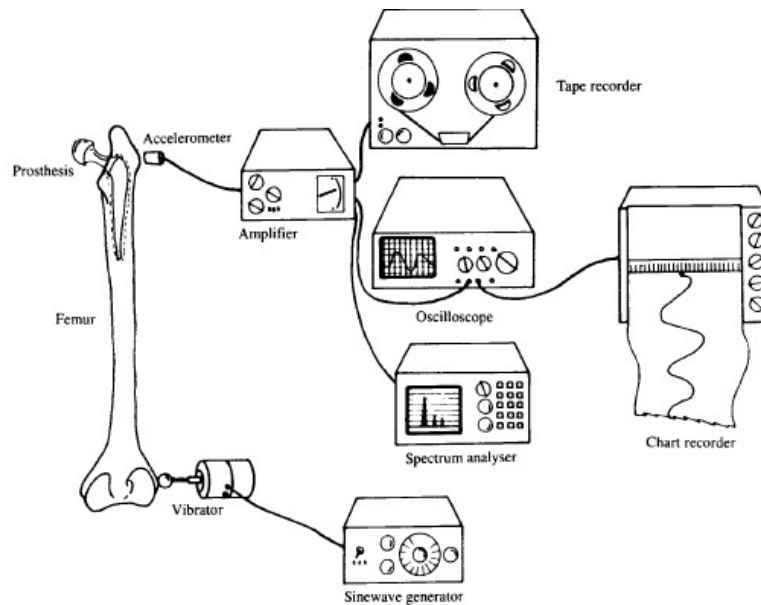


Figure 10: Equipment used for vibration measuring [82]

Li *et al.* [76] also studied this vibration technique using a shaker and accelerometer, and assessed the resonant frequencies of the secure and loose systems together with a spectral analysis, in different bandwidth frequencies. In addition, they analysed various examples of early and late loosening. Although the authors found evidence of macroscopic loosening in every seventeen specimens analysed, they also reported some wave distortion on a frequency range of 100-1200 Hz due to involuntary bone movements. As regards to the model capability in detecting early loosening, only in three of sixteen specimens micro loosening was detected.

The vibration method for bone-implant interface monitoring has clear advantages: it is easy to operate and capable of acting in different types of prosthesis. Also, it is able to diagnose loosening in about 13% more patients when compared to radiographs [77]. However, one can conclude that it is characterized by a significant number of limitations. The fact that the excitation and monitoring components are external to the implant, limits substantially the detected failure detected, due to the damping of the surround tissues of the interface. The use of a shaker restricts significantly the monitoring operation of osseointegration. Since extracorporeal excitation is required, the system cannot establish a controllable operation, and might affect regions outside the measuring range. A deeper analysis of the potential of vibrational technique was carried out by Qi *et al.* [78], through computer simulation, to reveal loosened femoral implants of total hip arthroplasty. It was concluded that the critical detectable failure size is of one-fifth of the stem length. In addition, it is likely to fail in detecting failures located at the stem central portion, which raises several questions in its ability to prevent critical loosening. The authors also advised the use of higher frequencies of excitation, at least 1000 Hz.

Rowlands *et al.* [68] tried to increase the area detected by vibration technique by using an ultrasound probe instead of an accelerometer. It appeared to be more accurate than previous vibration methods. It was able to detect input frequencies in a much wider range than the accelerometer, leading to enhanced detection of prosthesis loosening. Alshuhri *et al.* [79] performed a similar investigation for acetabular fixation investigation and was able to detect interface detachments of 2 mm with both the accelerometer and the ultrasound probe. Dahl *et al.* [80] used an electromagnetic shaker together with a Doppler ultrasound probe to detect the subsequent vibration in an Agility total ankle prosthesis. Cadaveric experiments were made, using a cemented prosthesis to simulate a fixed implant, and a press-fitted prosthesis to simulate a loose one. The use of an ultrasound probe proved to be able to measure differences in the resonant frequency for loose and tight implants. However, it is not specified the existing gap between the implant and bone, when a loose implant is measured. Further *in vitro* and *in vivo* experiments should be made to assess the viability of this method. A similar approach was made to analyse loosen states in total hip endoprostheses with an optical laser vibrometer together with an accelerometer [81]. It was concluded that the method was able to detect loosen states, for the saw model studied, mainly due to shifts in the resonant frequency. However, the authors did not explicit the interface condition, for a loosen implant. As the authors indicated, the magnitude values were strongly influenced by the quality of excitation, and they were unable to use this parameter to assess the state of the prosthesis. Further experiments are needed to validate this method.

Some concepts of inserting the vibration monitoring system into the implant, reducing the damping effect and consequently improving measurement results, were also studied. One of this methods was proposed by Puers *et al.* [82]. The authors implanted an accelerometer inside the hip implants' head, which then transmits the data by an embedded communication system comprising data conversion circuits and a telemetric link. The power to the sensor was projected to be provided by either a battery or an inductive link. Cadaver experiments were reported to give satisfying results. If the system is absent of loosening, a non-distorted sine-wave is captured, while if the implant is loosen the wave captured will behave in a non-linear manner. However, it is not detailed the capability of this system in detecting micro loosen states. Clinical tests were not conducted to determine the value of the system. Marschner *et al.* [83], [84], projected a new solution for the integration of a wireless measurement system for hip prosthesis, with and without an integrated femoral ball. The concept was composed of an accelerometer, a lock-in amplifier, a controller, a telemetry system, as well as a shaker external to the prosthesis (Figure 11).

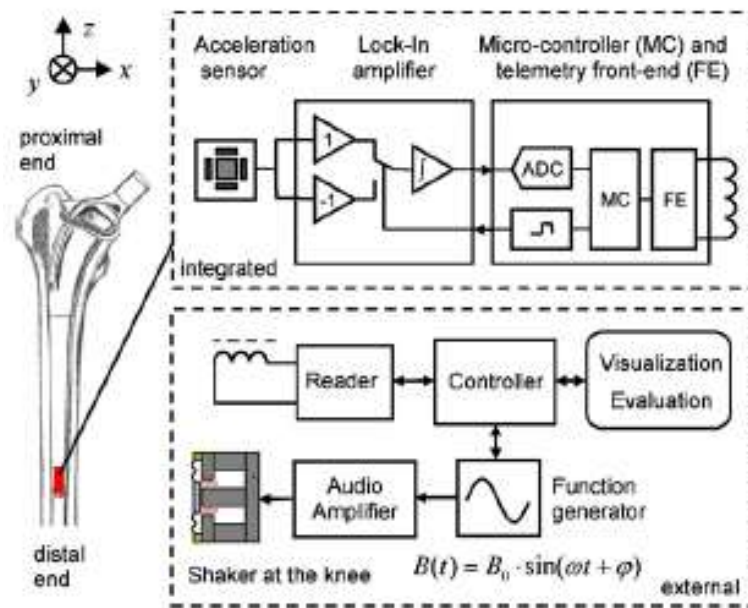


Figure 11: System concept of an embedded accelerometer [91]

More recently, Rieger *et al.* [85] suggested a new vibration method approach based on the use of external mechanical shockwaves by means of an expanding piezoelectric array, to propagate vibration up to 30 mm. Accelerometers were placed by bone pins in the cortical bone of the femur, to measure the resultant vibration and the consequent resonant frequency. This device is able to monitor several surfaces of the stem, providing that an accelerometer is nearby. However, as reported by the authors, complications arise when measuring the loosen state of the acetabular joint, since no significant resonance shifts occur. Besides, the use of external excitation does not allow a continuous operation of the monitoring system; and sensing operations outside instrumented implants may originate damping issues. *In vivo* investigation must still be conducted to validate this method. Analysing these mentioned methods of vibration, is possible to observe that, vibration method is capable of detecting bone-implant integration, and enable a controllable monitoring system with insignificant interaction in osseointegration. However, its ability in detecting micro loosening is still questionable, since most studies carried were *in vitro* and the interface gap distance is not explicit. Also, in some circumstances this method is not capable to overview the entire interface of the implant.

2.5.4. Acoustic Emission

Acoustic emission (AE) has been used as a useful method to investigate deformation and fissures in many materials. AE can be defined by a sudden release of energy within a solid, due to changes of initial state of the material, like for instance, a failure of fixation. Some of the energy dissipated comes in form of an acoustic (elastic) wave. Providing that this waves are of sufficient amplitude, they can be detected by a microphone or a transducer for example [86]. Shrivastava [87] reviewed the use of AE to monitor several bone conditions such as osteoporosis, strain and fracture healing process. He concluded that the first AE occurs initially in the plastic region, which means that is a viable method for fracture healing monitoring process. Davies J. [88] used this method to monitor the interface between cement and metal. The mechanical waves from interface fixation failure, were imposed into an AE transducer. The transducer resonated, converting the mechanical pulse into an electrical signal which was then transferred into a data acquisition board on a computer. The study revealed that this method can be used to evaluate the fixation state of implants. However, the authors had difficulty in interpreting the AE data obtained, because they were not able to differentiate between the cement cracking and de-bonding. Furthermore, in some cases they were unable to identify the location of the AE detected by the sensors. For an accurate monitoring, a significant number of AE sensors must be used, which reduces the flexibility of the concept, as well as its integration with the prosthesis itself. The same authors also proposed the use of emission and reflection ultrasonic waves [88], [89] to monitor bonded and debonded interfaces. The waves were emitted and captured by a transducer positioned over the interface (Figure 12). Accordingly to the characteristics of the reflected wave, the author could distinguish between a fixed prosthesis or a loosen interface. This method has several limitations. Firstly, as the authors indicated, if a fluid is present between a debonded interface it will be showed as bonded, due to the alteration of the reflected wave characteristic. Secondly, only *in vitro* tests were performed, which does not consider the damping effect of the surrounding tissues. In addition to these limitations, the use of a single transducer as pulse and echo capture, demands that the device must be positioned, correctly, normal to the cement/stem or stem/bone interface, which might be difficult to accomplish.

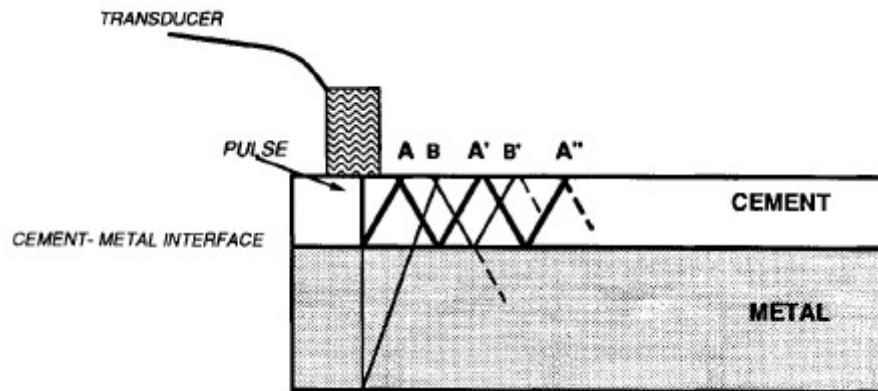


Figure 12: Ultrasonic transducer operation schematic [97]

Other suggested methods were based on resonance frequency monitoring [90], [91]. It consisted on providing a given impulse to the bone, by means of a hammer, and characterize the resultant frequency with a microphone. They intitled this method as resonance frequency monitoring (RFM). Since the concept was only experimented with cadavers, the validation of the approach is challenging. Considering that the use of the hammer is only for *in vitro* experimentation, one can only analyse the sensor device, which proven to be able to distinguish between loose and fixed interface. However, the use of an external sensor develops damping complications. Roques *et al.* [92] studied which parameter in an AE wave would be more suitable to identify loosening events. They concluded that the wave amplitude could not be used alone to monitor the interface. However, the appearance of high energy, associated with short rise times, could be linked to cracking or debonding. Mavrogordato *et al.* [93], developed a concept of AE sensors embedded within a hip stem, since former investigations used sensor mounted in the surface of the stem, which limits the signal obtained by the sensors and reduced the flexibility of the system. The system showed promising results for monitoring osseointegration in a continuous, non-invasive way. Cracks in the cement/stem interface were accurately detected, however, it was not proven to detect debonding effect. Further testing must be executed to prove the concept. Another study group [94] coupled the use of AE with piezo-crystals. The crystal was bound inside the implant and by exciting the system with an extracorporeal coil, it resonated generating ultrasound. The impedance resultant from a loosened or fixed prosthesis were then measured by an external coil. Unfortunately, very few *in vitro* tests were performed to evaluate this method. The use of an external detector and exciter is however of concern. Some acoustic sensor methods were proposed to detect acoustic events, such as squeaking during patient movement [95], [96]. They were consisted of 4 ultrasonic receivers, which were fixed, externally to the hip stem. However, squeaking may be caused by several undefined reasons and has not been proven to be related to wear, loosening or mispositioning [97]–[99].

Acoustic emission has three clear advantages: is non-invasive, capable of real time monitoring and, with the use of appropriate sensor, is possible to formulate a three-dimensional mapping of micro crack or de-bonding source location. The most significant complications of using AE, is the risk of occurring signal noise, which condition the process of monitoring osseointegration [93], [96]. As mention before, this method is incapable of distinguish between the occurrence of cracks on the cement and failure of fixation. Although it has been proven to be able monitor the appearance of fissures in the cement, its effectiveness in detecting lack of fixation is still questionable. The position of the sensors also conditions the monitoring process, considering that AE captured by one sensor is not able to locate the surface of de-bonding.

2.5.5. Magnetic Induction

Ruther *et al.* [100], [101] proposed two novel concept that uses magnetic sensors, which are excited by a coil, external to the implant. The magnetic sensors are composed of small metal spheres. These oscillators, are located in the surface of the stem, covered by a small membrane. After excitation, the magnetic sensors impinge on the small membrane. The first concept developed by the authors assessed the resultant velocity of the magnetic spheres which was captured by a detection coil. A loose implant tends to have a higher maximum velocity [100]. The limitation, reported by the authors, of using this method is the inability of controlling individually each single sensor of the stem, due to the use of an excitation coil. Also, they specified that there is a need to reduce the oscillators size in order to decrease their influence in the osseointegration process. In addition to these problems specified by the authors, it will be hard to monitor fixation before loosening occurs, since the sensors used do not cover the entire prosthesis. The same authors projected a similar monitoring system [101], [102], which analysed the sound emission of the oscillators, together with the vibration velocity. The signal emitted was captured by an accelerometer positioned on the skin surface. The schematics of the system are presented in Figure 13. *In vivo* experiments were made in rabbits to analyse the concept [103]. In this approach, similar problems arise. This method proves to be more sensible than former one. However, its ability in detection loosening before the prosthesis fixation fails, is also questionable, since it uses oscillators only in a portion of the stem. For an optimal monitorization to occur, several oscillators must be in place, which might condition the osseointegration of the system. The authors indicated that there is a need on reducing the size of the magnetic oscillators. Hereupon, this monitoring system is unable to fulfil the same requirement as the former concept.

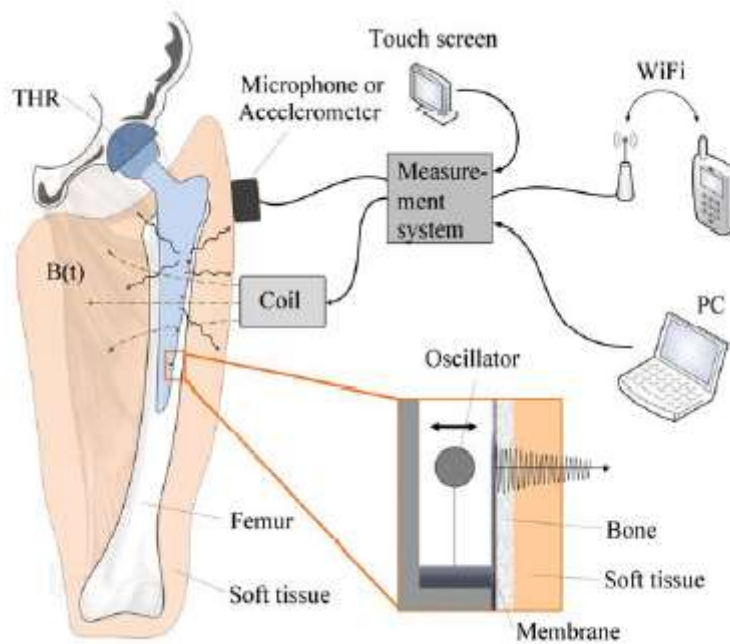


Figure 13: Magnetic induction system [109]

2.5.6. Electric Impedance

Bioimpedance has been studied through the years, as a method to characterize biological tissue [104]. Diverse components exist in the human body with different electrical properties such as organs, skin, fat, muscles, bones... Subsequently by applying a predetermined electric current to the biological system, it becomes possible to describe it by means of impedance, conductivity and permittivity. There have been some studies devoted to the use of electrical impedance imaging for representation of internal image, and to identify problems in the human body such as breast tumour [105]. Arpaia *et al.* [106], exploited electrical impedance spectroscopy as a new method to predict osseointegration. The author initially concluded that electrical impedance imaging did not provide enough resolution to be used for diagnosing the occurrence of loosening. Therefore, it was proposed an electrical impedance imaging based on variable polarization level. In their investigation, a sinusoidal stimulus was provided with different values of dc polarization and different fixation properties to a cow femur bone in one end, and in the opposing end the impedance was measured through relative voltage drops. The electrical stimulus was provided by an electrode (Figure 14). This *in vitro* experiment showed promising results in assessing osseointegration. To prove the concept the authors conducted an *in vivo* experiment in a cochlear implant [107]. The experiment showed “a high correlation between the osseointegration levels and the impedance magnitude”. With the concept proven both *in vivo* and *in vitro* the authors proposed a prototype microcontroller device to measure osseointegration by means of electrical impedance spectroscopy [108]. No further

developments were made regarding this method. The main concern of this approach is the invasiveness of the procedure. Due to the use of electrodes, the sinusoidal stimulus provided directly to the prosthesis might affect surrounding tissues or cause pain to the patient.

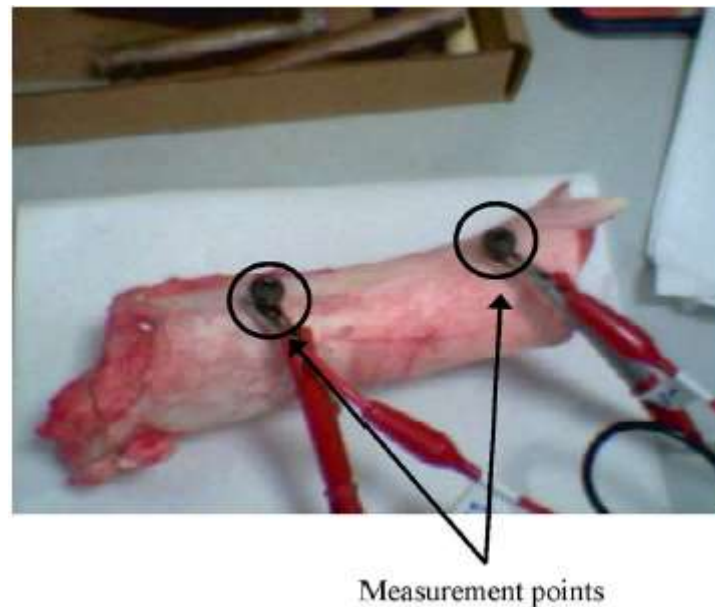


Figure 14: Schematic of the measuring system. The electrode induces electrical impedance [106]

2.5.7. Micromotion

There has also been some development on osseointegration monitoring devices using micromotion and migration measurement. Kärrholm *et al.* [109], concluded, by clinical observation, that early subsidence could be related to early revision prosthesis. Maher and Prendergast [110], used multiple linear variable differential transformers (LVDT) to compare loosening in several hip prostheses. A good precision can be obtained by using this measurement devices, however, it is very complicated to implant LVDT within an implant for *in vivo* measurement. Hao *et al.* [111] discriminated the use of a modified version of differential variable reluctance transducer (DVRT). The system consists on a pair of coaxial inductive coils and two pairs of variable resistors, connected in a way to form an RL-Wheatstone bridge. A small ferrite rod is inserted within the coils. The system is driven by a defined voltage and frequency. The movements of the induced rod are then monitored by the output voltage, providing a resolution of about 1 μm . *In vitro* tests were conducted [112], which were then discussed and the limitation of this process were investigated. The concept showed several problems in measuring large displacement values due to instrument errors and flux leakage. Also, since only bench tests were performed, the human body temperature was not considered which may have influence on the results. This concept is of hard evaluation since only few *in vitro* tests were made and the insertion procedure of the components was not fully described by the authors.

However, one can conclude that the viability of integrating every component inside the implant is questionable. In addition, this concept is not able to monitor various regions of the interface between stem and bone, thus a significant number of monitoring systems would have to be used for an optimized operation.

2.5.8. Strain

There has been some investigation on *in vivo* strain monitoring. The main default device used to measure strain are strain gauges. Fresvig *et al.* [113] suggested the use of optical Bragg grating fiber to evaluate the strain values. Fiber Bragg reflects to the core particular wavelengths of light and transmits all others. If the fiber is strained, the wavelengths are shifted and measured as related to the level of strain applied. *In vitro* tests were made to validate the concepts together with incorporated strain gauges. The study showed promising results in identifying deformation in bone. Lajnef *et al.* [114] based their concept in integrating piezoelectric polymer transducers, together with floating gate injection to measure growing stresses in implants. It showed a correlation between the fatigue measured and the number of stress cycles experienced by the structure. Alpuim *et al.* [115] used a combination of piezoelectric and piezoresistive materials as a strain sensor. Through changes of electric relative resistance, they were able to monitor the strain values applied. A sensitivity of 30 mV/ μm was achieved. McGilvray *et al.* [116] developed a locking plate with a sensor incorporated, capable of monitoring bone fracture healing. These methods proven to be able to measure the incident strain continuously, with a minimal interaction between the surrounding tissue. Nonetheless, strain monitoring systems can only be used to assess bone healing event and thus it can't be used as a solely methodology to analyse interface fixation.

2.5.9. Other Identification Methods

Although it is not an instrumented way of monitoring, serum markers can be an efficient way of detecting loosen states. One can analyse biological markers to detect the increasing number of biomolecules involved during fixation failure, and, therefore, prevent loosening. There have been evidences that the synthesis of nitric oxide (NO) can be related to the occurrence of wear debris and, thus, implant loosening [117], [118]. The incidence of osteolysis and the absorption of wear debris produces signal molecules responsible for the production of NO. This molecule has several functions, such as blood pressure regulator. Stea *et al.* [119], suggested, through *in vivo* tests on patients admitted for revision surgeries, that with severe loosening and with plastic or metal wear debris, a higher percentage of inducible NO synthase enzymes (iNOS) appear. To prove this concept Steinbeck *et al.* [120], investigated the relation between oxidative stress (caused by wear debris) and

osteolysis. The authors analysed and quantify, using immunostained techniques, the amount and relation between them, of five oxidative elements that developed around the stem, osteolysis, inflammation and wear debris. Important conclusions were made. Firstly, they found a strong relation between inflammation and wear debris. However, they did not relate with the degree of osteolysis. Secondly, it was observed that bone resorption is related to oxidative stress. Finally, a strong correlation was found between the degree of osteolysis and the amount of three oxidative factors: cyclooxygenase-2 (COX2), high mobility group protein-B1 (HMGB1) and 4-hydroxynomenal (4-HNE). Also, similarly to Stea *et al.* [119], an accumulation of iNOS was discovered. Other serums were studied with promising results. Granchi *D. et al.* [121] suggested osteoprotegerin, (OPG), which is produced as a regulator and protective mechanism for bone loss, as possible marker for aseptic loosening. Landgraeber *et al.* [122] evaluated the increase of tetracycline-resistant acid phosphatase 5b (TRAP 5b) and C-terminal telopeptides of type I collagen (CTX) serum in patients with aseptic loosening. CTX proven to be a poor marker. On the other hand, TRAP 5b levels on patients with aseptic loosening were significantly higher than the control ones. A sensitivity of 83,3% was obtained. Remain unsolved how to embed monitoring systems based on detection of biological markers within implants and without minimal interaction with the bone-implant interface.

2.6. Comparison among osseointegration sensors

Considering all limitations found on already proposed osseointegration monitoring systems, an improved technology will require to:

- (1) Operate non-invasively and with minimum interaction with peri-implant tissues;
- (2) Allow stretchable and flexible integration inside implants;
- (3) Allow their design with different topological structures and geometry;
- (4) Enable controllable and personalized monitoring to various target regions of the tissues;
- (5) Operate as therapeutic actuators;
- (6) Allow identifying bone-implant integration states before damage, including topological identification.

Having described past methods used to detect loosening states, a comparison is mandatory to identify the not fulfilled requirements for each procedure (Table 4). It is of note that marker techniques, were excluded from evaluation, since they are characterized in a different category of the one studied in this work. This section focus only on instrumented monitoring systems capable of

preventing and detecting interface loosening, in postoperative manner. Although they were here described, further reviews should be made to evaluate marker techniques.

The table presented is divided into six different methodologies categories. Each method described previously, is assigned a giving category according to the projected approach. The methods are summarized in conformance to the variable signal or device that excites the monitoring system, and the sensor that identifies and measures the emitted indicator. This table shows that no osseointegration monitoring system was proposed to date, with ability to be incorporated within instrumented bone implants, such that outstanding performance and long-term success of joint replacements can be ensured.

Methodologies	Method	Requirements					
		(1)	(2)	(3)	(4)	(5)	(6)
Vibration	External Electromagnetic shaker/External accelerometer [74], [76], [77], [79]	✓	✗	✓	✓	✓	✗
	External Electromagnetic shaker/External ultrasound probe [68], [79], [80]	✓	✗	✓	✗	✓	✗
	External Electromagnetic shaker/External laser [80], [81]	✓	✗	✗	✗	✓	✗
	External Electromagnetic shaker/Internal accelerometer[81]–[84]	✓	✗	✓	✗	✓	✗
	External Shockwaves/Internal accelerometer [45]	✓	✗	✗	✓	✓	✗
	Piezoelectric actuator/Piezoelectric sensor [75]	✓	✗	✗	✗	✓	✗
	Mechanical loading/AE transducer [88]	✓	✓	✓	✗	✗	✗
	Mechanical loading/Ultrasonic transducer [88], [89]	✓	✓	✓	✗	✗	✗
	Mechanical loading/Microphone [90], [91]	✓	✗	✓	✗	✗	✗
	Mechanical loading/Embedded AE sensors [93]	✓	✓	✓	✗	✗	✗
Acoustic Emission	External coil/Piezo crystal [94]	✓	✓	✗	✗	✓	✓
	Mechanical Loading/Ultrasonic receiver array [95], [96]	✓	✗	✗	✓	✗	✗
	Magnetic force/Detection coil [100]	✗	✗	✗	✗	✓	✗
	Magnetic force/Accelerometer [101], [102]	✗	✗	✗	✗	✓	✗
Electrical Impedance	Electromotive force/Dielectric Spectroscopy [71]	✗	✓	✓	✓	✓	✓
	Displacement/Linear Variable Differential Transformer [110]	✗	✗	✗	✗	✗	✓
Micromotion measurement	Displacement/Variable Reluctance Transducer [111]	✗	✗	✗	✓	✓	✓
	Strain/Bragg Fiber [113]	✓	✓	✓	✓	✓	✗
Strain measurement	Strain/Strain Gauges [113]	✓	✓	✓	✓	✓	✗
	Strain/Piezoelectric with floating gate transistor [114]	✓	✓	✓	✓	✓	✗
	Strain/piezoelectric sensor [115]	✓	✓	✓	✓	✓	✗
	Electromagnetic wave/Resonance Response Frequency [116]	✓	✓	✓	✓	✓	✗

Table 4: Comparison of instrumented loosening monitoring systems

3. Methods

In vitro studies were made to prove the new concept of osseointegration monitoring using cosurface capacitors integrated on RLC resonant circuit. In this chapter, a complete description of the method developed to analyse the concept is made. To carry out the analysis, a test apparatus was developed for *in vitro* evaluation. This experimental apparatus had to be capable of electromagnetically simulate the bone-implant interface for different interface scenarios. To accomplish a functional sensing device a printed circuit board (PCB) was produced. In the next chapters, the measuring method will be described in detail.

3.1. Detection method

The detection method used in this work uses capacitance variations to monitor interface changes. The following RLC circuit (Figure 15) was used to measure capacitance variations.

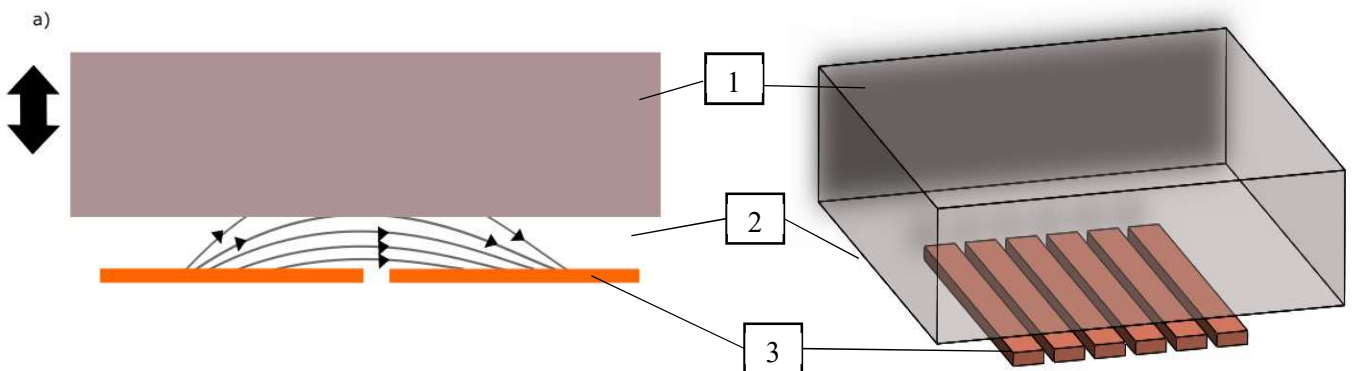
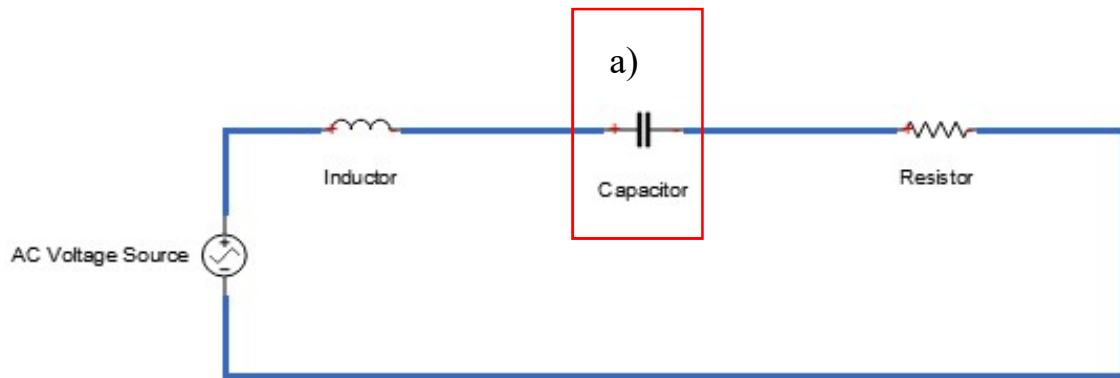


Figure 15: Schematic of the capacitive sensor for interface monitoring. 1. Bone portion; 2. Dielectric (The dielectric includes the area/volume above the electrodes (3)); 3. Electrodes

By exciting electrodes with a voltage signal, the dielectric is stimulated by electric and magnetic fields. These electrodes act as the capacitor of the circuit. By changing the dielectric substance, the permittivity of the environment will alter and so will the capacitance of the system. Embedding a sensor of this type in the surface of implants, it is safe to conclude that it reveals a given capacitance when the medical device is osseointegrated and a distinct one for loosening states. The differences from each capacitance can be examined through the resonant frequency at each given state. The lower the capacitance the higher the respective resonant frequency. This sensitivity assures, theoretically, that this method holds potential to detect small detachments of implants-bone interface.

In a series RLC circuit, at the resonant frequency the impedance is at its minimum value. Consequently, the voltage across the resistor will increase to its maximum value. This effect can be observed by calculating the amplification ratio in the resistor. In Figure 16, the voltage ratio between the output voltage signal (at the terminals of the resistor) and the input voltage signal, are plotted with the corresponding frequency.

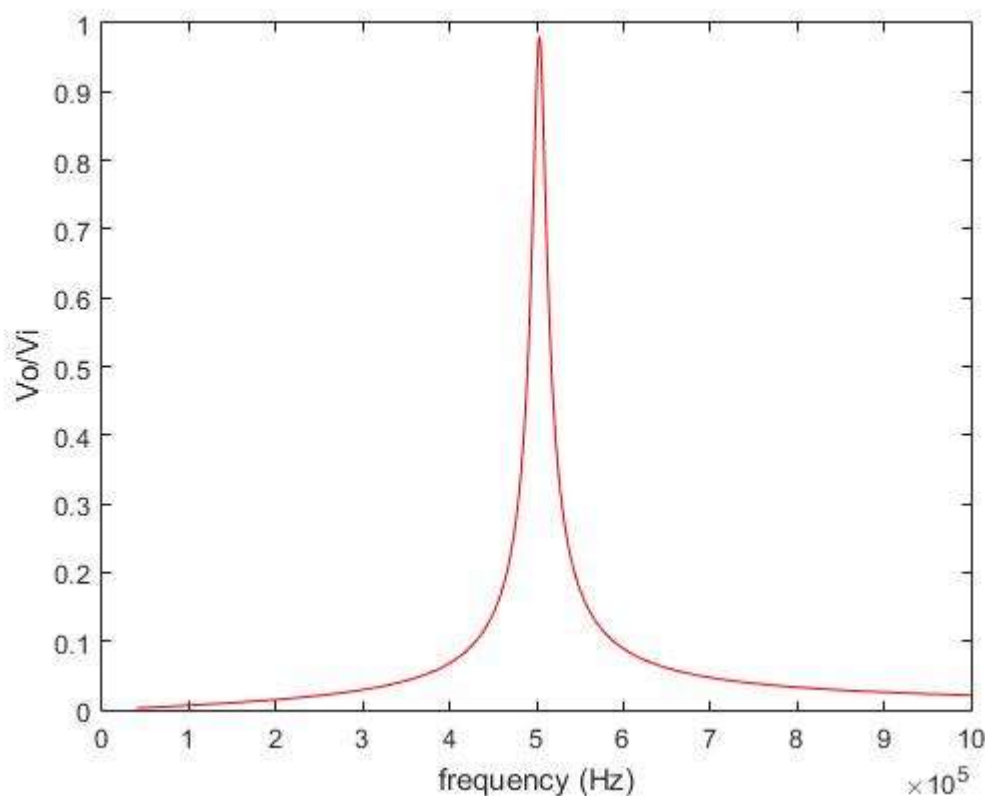


Figure 16: Example of a voltage ratio as a function of frequency in a RLC circuit ($L=10$ mH, $C=10$ pF, $R=1$ k Ω). A resonant frequency is about 500 kHz.

This means that by analysing the frequency spectrum and capturing the signal in the circuit's resistor, the maximum tension and the corresponding resonant frequency can be obtained. Since the capacitance shifts with the relative position of the bone to the cosurface electrodes, the resonant frequency will also shift, according to Equation 1, however, the maximum amplitude of the signal remains with the same value.

$$w = \frac{1}{\sqrt{LC}}, \text{ for } X_C = X_L \quad (1)$$

For instances, if the bone is positioned directly above the electrodes, a given resonant frequency can be observed by obtaining the maximum value of the output signal. When the bone is moved away from the sensor the waveform will shift, resulting in a new capacitance and resonant frequency. In this work, a mean resonant frequency of around 384 kHz was registered for a fixed prosthesis. The dielectric of the system can also be measured through phase changes. At the resonant frequency, the admitted signal is in phase with the signal captured from the resistor. This event can be observed in Figure 17, where the argument of the electric impedance was plotted with the frequency. For this example, the resonant frequency is around 500kHz. When resonant frequency shifts so will the phase between in/out signal. The capacitance can then be obtained by the following formula:

$$\tan(\varphi) = \frac{(X_L - X_C)}{R} \quad (2)$$

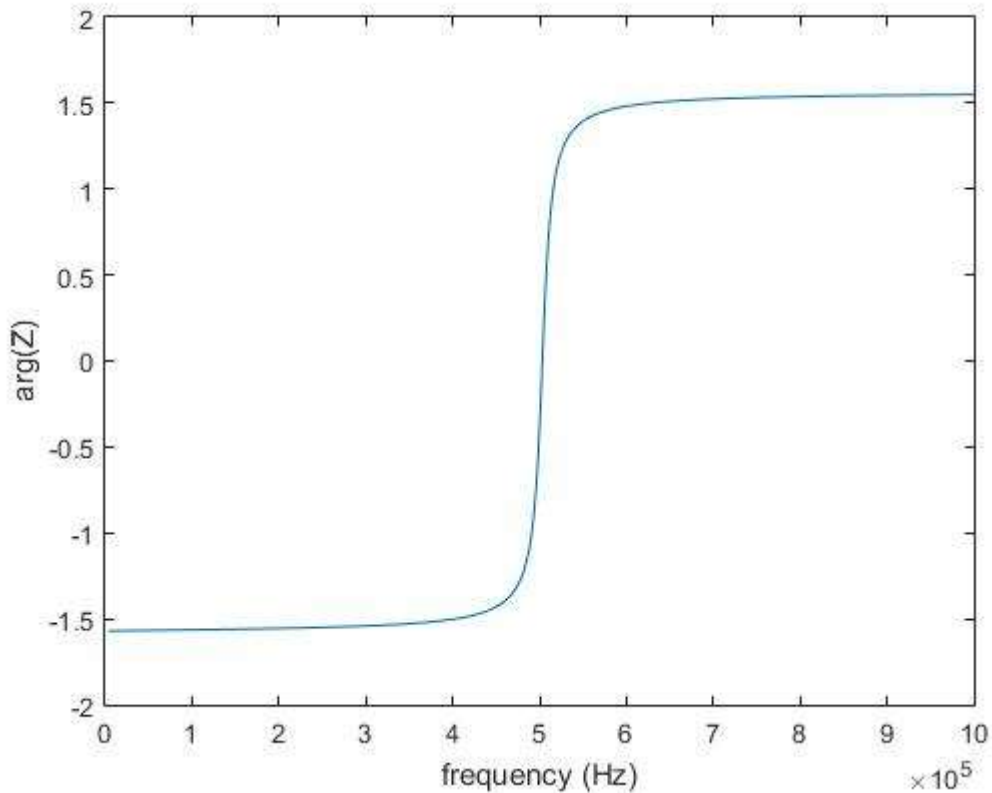


Figure 17: Phase shift in a RLC series circuit, for a resonant frequency of about 500 kHz.

3.2. RLC circuit development

For each given interface, the maximum electric tension was examined and the correspondent resonant frequency was recorded. The capacitance deviation values were also evaluated through phase differences between the admitted tension, and the signal obtained in the resistor. So that variations of capacitance and phases could be perceived, the components of the circuit had to be chosen accordingly. Upon the choosing of each component, the circuit was tested using both an oscilloscope and a signal generator. For this work, measurements were first made with only a bone portion. Then, to simulate an intrinsic implant, the bone was previously submerged into a saline solution.

3.2.1. Electric components selection and capacitance review

First the capacitance of a bone was investigated. Figure 18 represents the capacitance of a wet bovine bone in the axial, radial and circumferential directions as a function of frequency.

Analysing this behaviour, it is possible to conclude that bone capacitance decreases with the increase of capacitance.

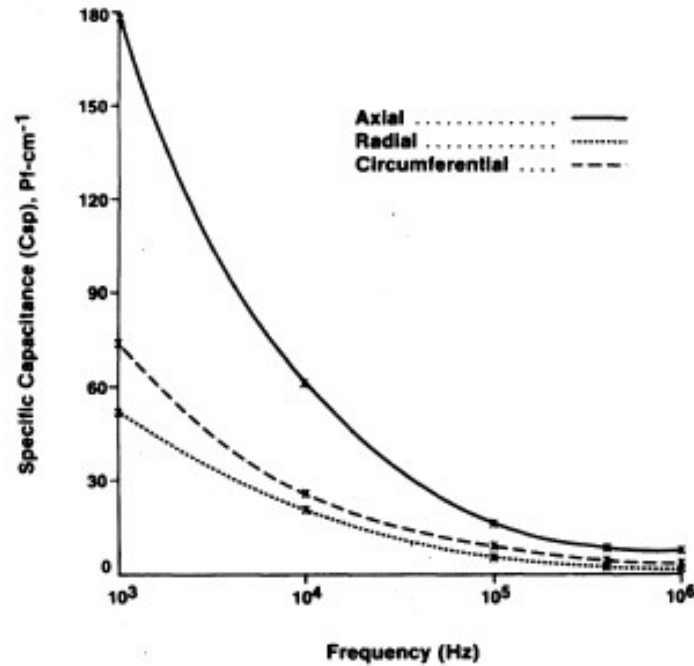


Figure 18: Capacitance of wet bovine bone as function of frequency in axial, radial and circumferential directions [130]

The capacitance found to produce this graphic was obtained with parallel plates, which is different from the setup used in this work. A previous study with a setup similar to the one in this work was difficult to find. Therefore, the graphic shown in Figure 18 serves only to demonstrate that the capacitance measured is expected to be in the order of the micrometres.

The choice of the inductor only influences the resonant frequency (equation 1). The value of the inductance together with the size of the inductor were the criterion used for the choosing of this component. It needed to have a high inductance for low resonant frequencies, but specifications of instrumented implants require small size components. An inductor of 10mH was then chosen.

The selection of the resistor applicable to this RLC circuit influences the bandwidth and quality factor. The equipment used during experiment does not allow the use of a circuit with a high-quality factor, since it's resolution is relatively small. The bandwidth of the signal obtained, also had to be large enough so that differences between small interface shifts could be perceived. Thus, a resistor of 1000 Ω was used. With this component a bandwidth of around 15 kHz was obtained.

To understand how the capacitance would alter when the bone was formerly submerged into a saline solution, the capacitance of the fluid had to be investigated. To obtain the capacitance of the saline solution Stogryn [123] equations were used. He developed equations of the Debye form for

calculating the dielectric constant for saline solution as a function of temperature and salinity. Using a salinity value of 9 part per thousand (ppt) and a temperature of 25°C, a value of 80 was obtained for the dielectric constant. The capacitance was then calculated using the formula for static electric fields:

$$C = \epsilon_r \times C_0 \quad (3)$$

The obtained capacitance of the saline solution was 7 pF.

3.3. Printed circuit board preparation

With the components selected, a printed circuit board was designed according to the size of the components and the restrictions of test structure. In Figure 19 and 20 the board design and the finished PCB can be observed respectively.

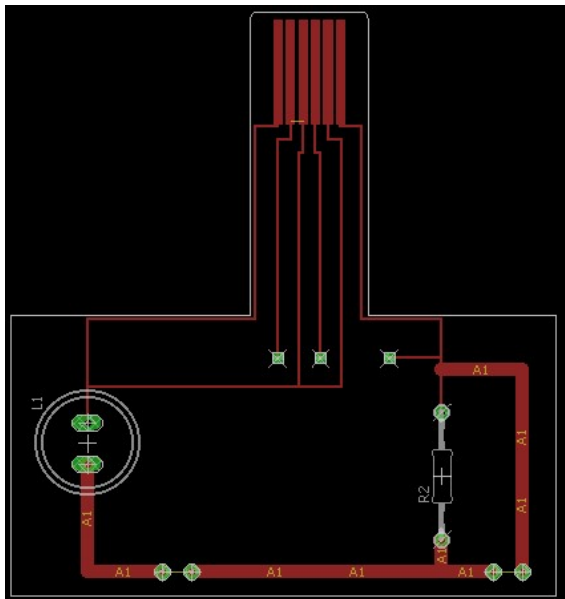


Figure 19: Schematic of the PCB design (image taken from Eagle 8.1.0 free version). L –10 mH inductance; R – 1 kΩ resistor;



Figure 20: Produced PCB

External copper wires were used to connect the signal generator and oscilloscope. The copper tracks were designed to be as small as possible and as far as possible from each other to reduce unwanted capacitances. The PCB with the welded electric components is displayed in Figure 21.

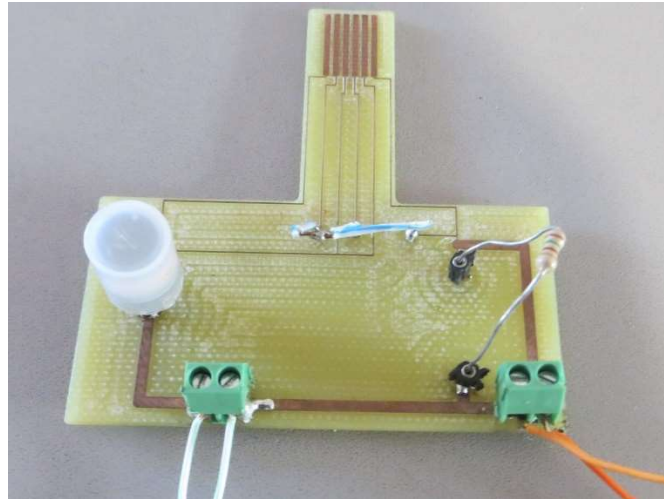


Figure 21 Finished PCB with welded electric components

3.4. Experimental apparatus

Several specifications had to be fulfilled so that the *in vitro* experiment apparatus mimics a monitoring system, embedded within an instrumented implant, surrounded by a bone structure. The following requirements were taken into consideration upon the design of the experimentation system:

- (a) A small portion of bone must be used to prove the concept. An apparatus must allow relative micro-scale movements between this bone segment and co-surface electrodes
- (b) The stimulators need to be as close as possible to the bone portion when absent loosening is intended.
- (c) To replicate the surrounding conditions of the human body, the interface must be surrounded by an isotonic saline solution. However, the cosurface electrodes can't be in contact with the fluid.
- (d) It must be adaptable to different size cosurface capacitive system, and the substitution must be made in an accessible and easy way.

To fulfil conditions (a) and (b) a multi-test machine was used. This machine used provides accurate vertical positioning with high accuracy ($\pm 0,1\%$ of indicated value or $\pm 0,01 \mu\text{m}$, whichever is larger). The multi-test machine is exhibited in Figure 22.



Figure 22: Multi-test machine

An adjuvant system was designed to support every component needed to carry out the experiment. In Figure 23 the assembly design of the system is presented.

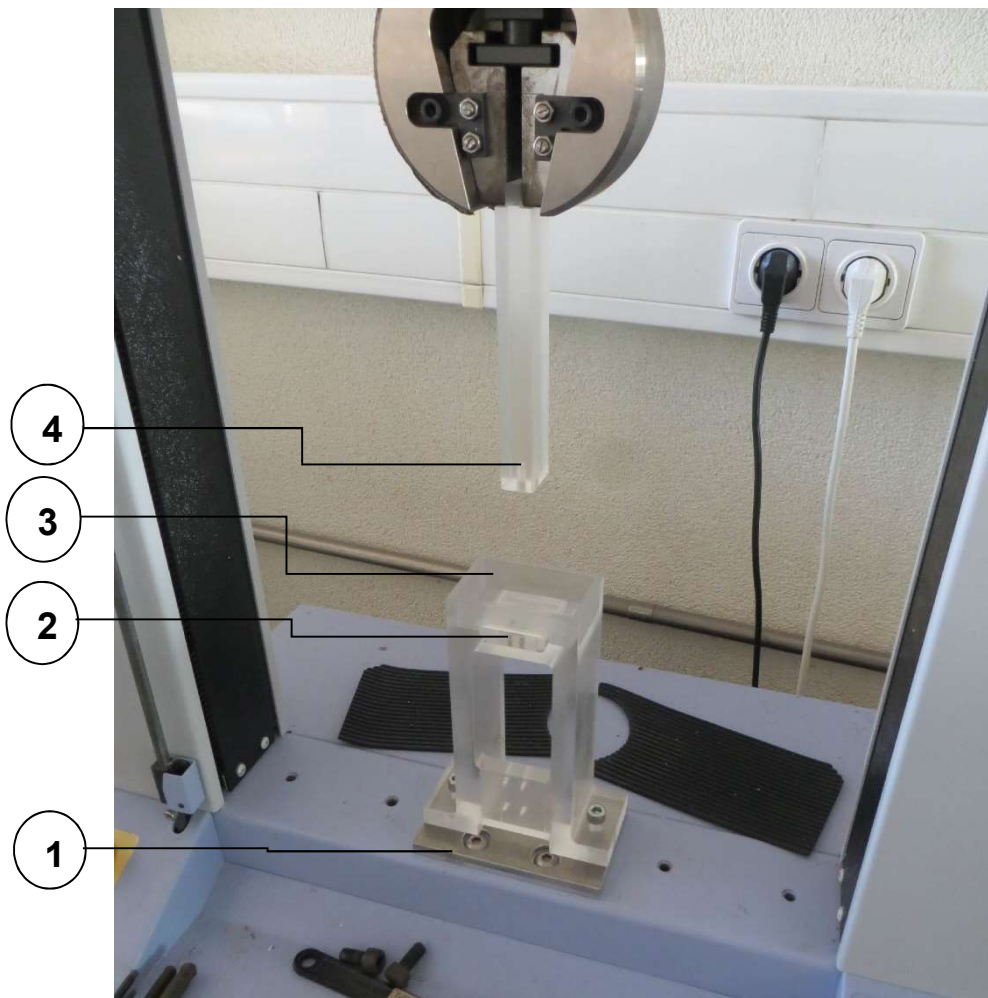


Figure 23: Final assembly of the experimental apparatus.

Each different component is numbered from 1 to 4. The description of each component is given:

- (1) To ensure the stability of the structure and to fix it to the multi-test machine, an aluminium board was machined according to the connection holes of both the structure and the multi-test machine. The dimensions of the board are 130x80 and 10 mm of thickness. Aluminium was chosen due to costs, malleability and stiffness.
- (2) The test board represented in (2) was designed with the intention to embed the cosurface capacitive system. The dimensions of it are 40x42x10 mm with a 2mm depth to enclose the cosurface electrodes. The board is made from acrylic, the choosing of the type of material will be explained later. In Figure 24 the board can be more clearly viewed. Two holes were made to lodge two small screws.



Figure 24: Part (2) of the experiment structure

- (3) The main structure of the test assembly is made of acrylic and it was designed to fulfil every requirement needed for the experiment. Holes were machined to connect it to component (1). The upper part of the structure is open with 20 mm of depth as it is presented in Figure 25. This container shaped structure is meant to contain the saline solution, to guarantee condition (c). The square part of the upper surface represents a small shell with 1 mm of thickness. The hollow part on the front side of the structure is where the test board (3) will be fixed. The dimensions of this “window” are the same as the test board to reduce gap dimensions. To ensure that the only gap between both structures is the thickness of the shell, two screw holes were machined and two pins were screwed, with purpose to compress the PCB onto the bottom part of the shell. This shell or case was made to protect the test board from the saline solution. The aim of the handles made in (2) is to remove it from the hollow feature, to replace or correct the stimulators. This ensure the adaptability of the system and consequently requirement (d) is accomplished.



Figure 25: Part (3) of the experiment structure

(4) In this “claw” chapped part, the bone will be fitted. The bone will be clamped using two nylon screws as it can be seen in Figure 26. The dimensions of the gap between each plate of the acrylic claw is of 40 mm. This component is screwed in a long acrylic plate to detach the conductive components of the multi-test machine from the cosurface capacitive system. The intention is to minimize the influence of the metal components, such as the metal claw, of the multi-test as a measured dielectric. The upper part of the structure was machined so that it could be clamped to the multi-test machine. This part was also made of acrylic to reduce dielectric influence.



Figure 26: Part (4) of the experiment apparatus

The whole assembly was made so that the test board (part 2), is centred in respect to the bone portion (part 4). One of the limitations of this process is that, when the aim is to evaluate a fixed implant, that is, when the bone is in contact with the upper part of structure (3), it is not possible to guarantee that the bone is, in fact, in contact with the structure; or, because of the topological structures and textures of bone, if the aim is to evaluate a loose implant, it is not possible to guarantee that the bone is indeed not in contact. The whole structure is made of acrylic to diminish its influence on the measured signal.

3.5. Experimental procedure

The signal was emitted through a signal generator and captured with the use of an oscilloscope. The equipment is exhibited in Figure 27.

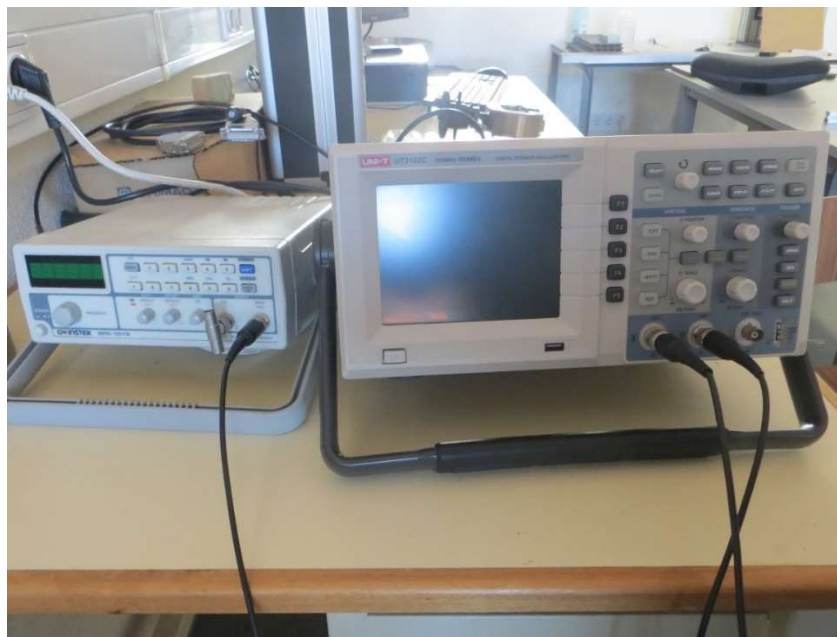


Figure 27: Equipment used for generating the input signals and measure the output signals. Left: Signal Generator, Right: Oscilloscope.

The signal generator is a SFG-1013, function generator from SFG-1000 series, GW Instek. It provides an accurate frequency from 0.1 Hz up to 3MHz. The oscilloscope showed in the image is a digital storage oscilloscope UT3012C.

The PCB was placed in the board (part (2)) and the board was inserted in the slot of the test structure. The screws from part (2) were screwed to assure complete contact between the PCB and the upper part of the isolating shell. This setup can be observed in Figure 28.

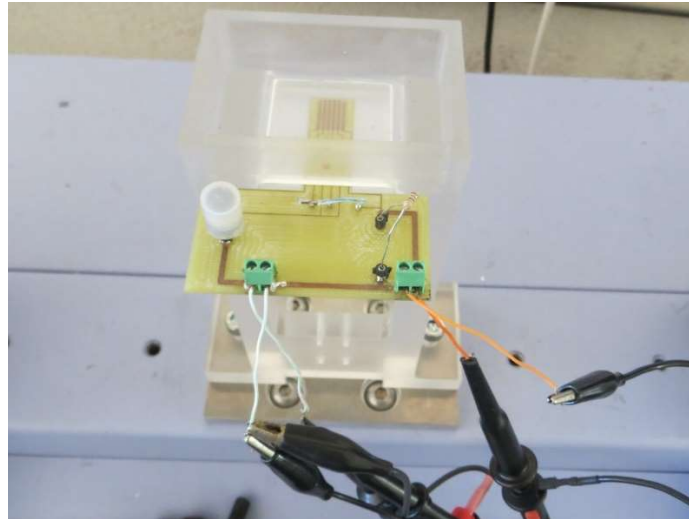


Figure 28: Measurement setup.

First a small bone portion was cut and prepared ($\varnothing=25$ mm). In Figure 29 the bone portion is depicted.



Figure 29: Bone portion measured

It was then placed inside the claw shaped part (part 4) and fixed with the aid of the nylon screws. A special attention was given to assure that the bone was firmly fixed.

To comprehend how the dielectric diverged, different interfaces were assessed. First the bone was pressed onto the structure with a non-zero force equal to 2 N to simulate a fixed prosthetic and

to guarantee that the bone has its overall surface as close to the sensor as possible. From this starting position, incremental micro-displacements of the bone were carried out. For each interface, the voltage amplitude in the oscilloscope was measured, as well as the corresponding resonant frequency from the signal generator. The bone was raised 5 microns 20 times until it reached 100 microns. For each 5 microns, the resonant frequency was measured using the procedure previously described. This procedure was redone by progressively increasing the distance from the sensor to 10, 50 and 100 micro each analysis.

For each point, the phase shift of the resistor waveform in respect to the entry signal was also measured. Between each series of experiments, the bone was submerged into a saline solution for a few minutes, fixed to the structured and the whole procedure was then repeated. In the next chapter, the results are showed.

4. Results

4.1. Capacitance variations without saline solution.

4.1.1. By measuring the resonant frequency

For each different increase in distance (Δy), 3 repetitions were made. The result for the capacitance measurements with a bone without serum, as a function of the relative displacement between the bone and the cosurface capacitive system are presented in Figure 30. The graphic depicts every set of 20 measurements for each different gap interval. In these measurements only shifts of 10 Hz were registered. In every experiment, the bone pressure can be assumed to be inexistent from around 50 μm .

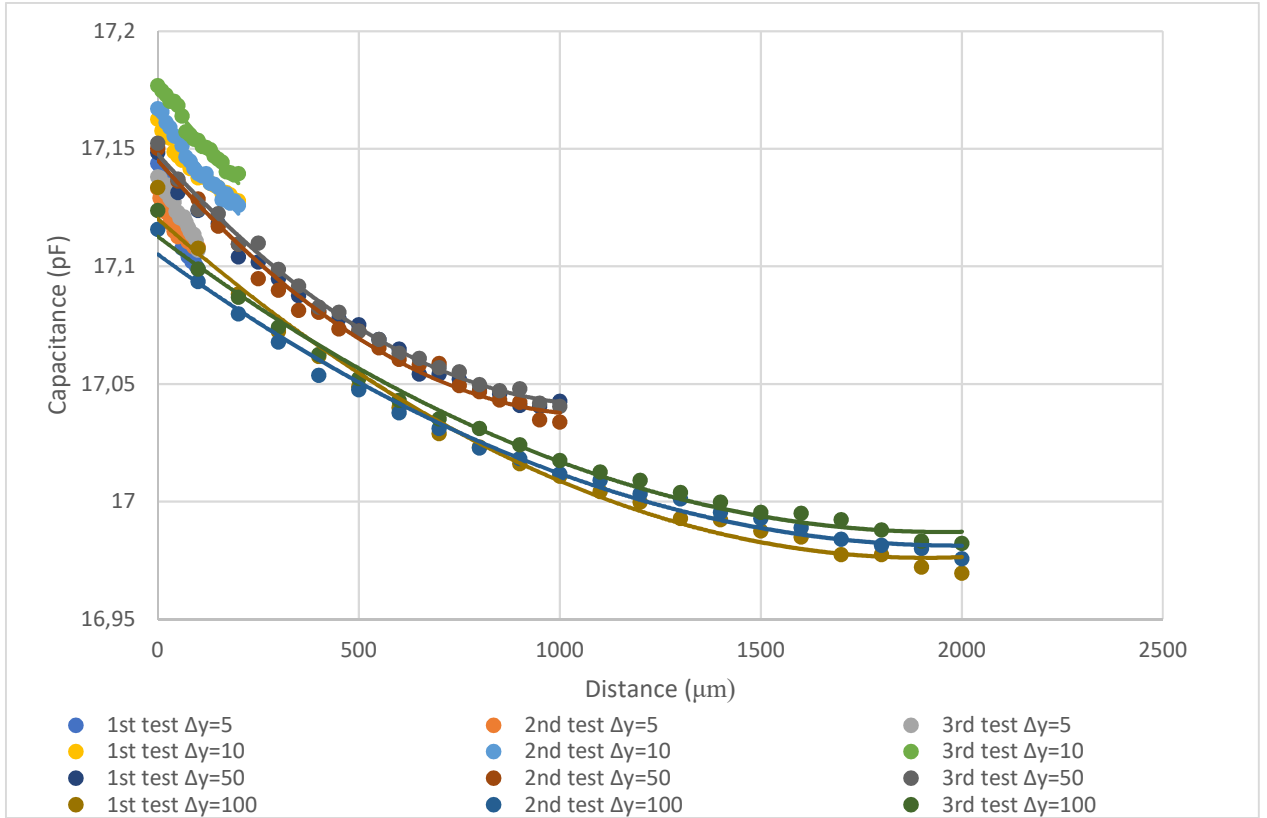


Figure 30: Results measured through resonant frequency measurement, for a bone free of serum

Observing these results, it is clear that the measured capacitance decreases with increase of distance. Tracing a tendency line over the larger interval measurements, it is possible to conclude that the decay of capacitance can be described by a quadratic polynomial. Which means that with the increase of distance from the cosurface capacitive system to the bone, the capacitance tends to a null slope. Analysing the first point in each attempt, (when the bone is pressed onto the measurement structure) the capacitance varies between 17,116 and 17,177 pF. The corresponding tendency lines equations and coefficient of determination (R^2) for a Δy equal to 50 and 100 μm , for each series of tests, are described in Table 5.

Δy [μm]	Test number	Tendency line equation	R^2
50	1 st test	$C = 8 \times 10^{-8} d^2 - 0,0002d + 17,143$	0,9939
	2 nd test	$C = 9 \times 10^{-8} d^2 - 0,0002d + 17,145$	0,9892
	3 rd test	$C = 8 \times 10^{-8} d^2 - 0,0002d + 17,148$	0,9947
100	1 st test	$C = 4 \times 10^{-8} d^2 - 0,0002d + 17,120$	0,9884
	2 nd test	$C = 3 \times 10^{-8} d^2 - 0,0001d + 17,105$	0,9901
	3 rd test	$C = 3 \times 10^{-8} d^2 - 0,0001d + 17,113$	0,9910

Table 5: Quadratic tendency line equations for $\Delta y=50 \mu\text{m}$ and $\Delta y=100 \mu\text{m}$, through resonant frequency measurements, for a bone free of serum.

As previously described, X-rays can't distinguish distances of 700 μm , thus it is important to evaluate how capacitance alter for distances smaller than this limit. Adjusting the previous results to a distance interval between 0 and 200 μm , a series of measurements with a larger linearity can be obtained. The measurements for these experiments are showed in Figure 31, with a linear tendency line over each series of measurements.

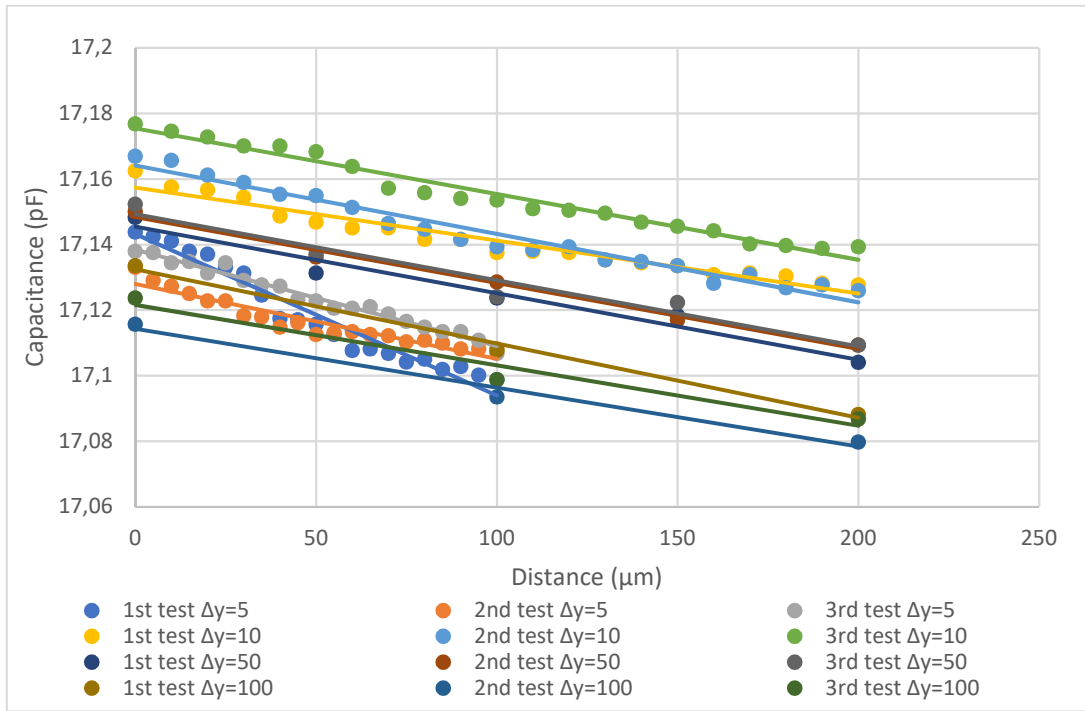


Figure 31: Adjusted results between 0 and 200 μm , for measured resonant frequency in a free of serum bone

Table 6 describes each corresponding linear regression each experiment made between 0 and 200 μm

Δy [μm]	Test number	Tendency line equation	R^2
5	1 st test	$C = -0,0005d + 17,143$	0,9541
	2 nd test	$C = -0,0002d + 17,128$	0,9064
	3 rd test	$C = -0,0003d + 17,138$	0,9798
10	1 st test	$C = -0,0002d + 17,157$	0,9513
	2 nd test	$C = -0,0002d + 17,164$	0,9659
	3 rd test	$C = -0,0002d + 17,175$	0,9704
50	1 st test	$C = -0,0002d + 17,145$	0,9644
	2 nd test	$C = -0,0002d + 17,148$	0,9897
	3 rd test	$C = -0,0002d + 17,149$	0,9533
100	1 st test	$C = -0,0002d + 17,133$	0,9937
	2 nd test	$C = -0,0002d + 17,114$	0,9819
	3 rd test	$C = -0,0002d + 17,122$	0,9607

Table 6: Tendency linear line equation for the measured results, for resonant frequency measurement, in a bone free of serum

A similar slope is seen in each equation. The mean slope in this analysis is about $0.00023\text{pF}/\mu\text{m}$, which means that the average variation of capacitance per micrometre measured is of 0,23 femtofarad.

4.1.2. By measuring phase shift

An alike analysis will be made for the capacitances measured through phase shifts. Figure 32 shows the measurements obtained. In these measurements, only changes of 5 ns were perceptible. Only 2 attempts were made for each different distance interval.

The tendency lines can once again be estimated through quadratic equations. Table 7 indicates the tendency line equations and the matching coefficient of determination.

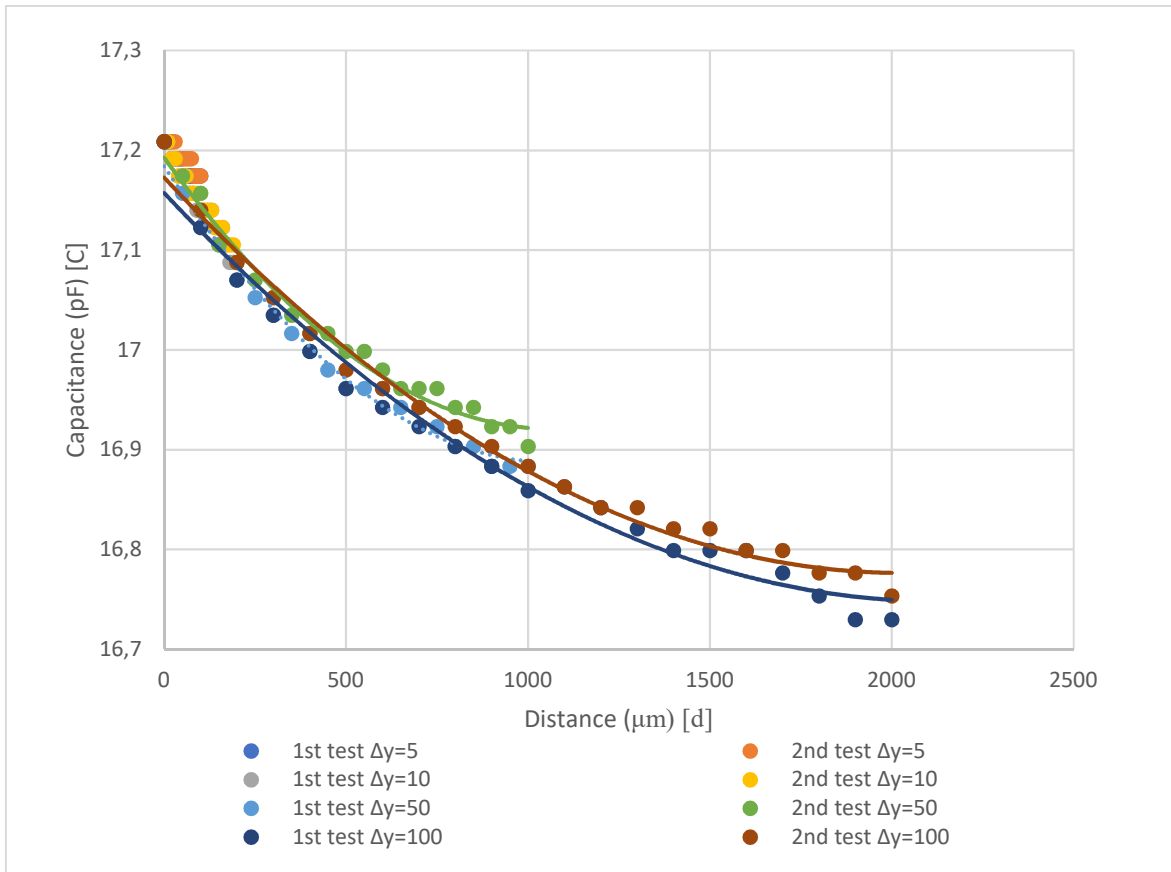


Figure 32: Results measured through phase shifts, for a bone free of serum

Δy [μm]	Test number	Tendency line equation	R^2
50	1 st test	$C = 3 \times 10^{-8} d^2 - 0,0005d + 17,035$	0,9874
	2 nd test	$C = 2 \times 10^{-7} d^2 - 0,0005d + 17,043$	0,9844
100	1 st test	$C = 9 \times 10^{-8} d^2 - 0,0004d + 17,011$	0,9789
	2 nd test	$C = 9 \times 10^{-8} d^2 - 0,0004d + 17,017$	0,9885

Table 7: Quadratic tendency line equation for the measured results, through phase shifts, for a bone free of serum

A similar pattern was found: increasing distances imply the quadratic term to decrease. Which again verifies that for distances over 1000 μm , the capacitance leads to a decrease in slope thus reducing shifts in capacitance. Limiting the observable interval from 0 to 200 μm , the data obtained can once again be approximated with a linear tendency line. In Figure 33 the graphic is adjusted to this interval.

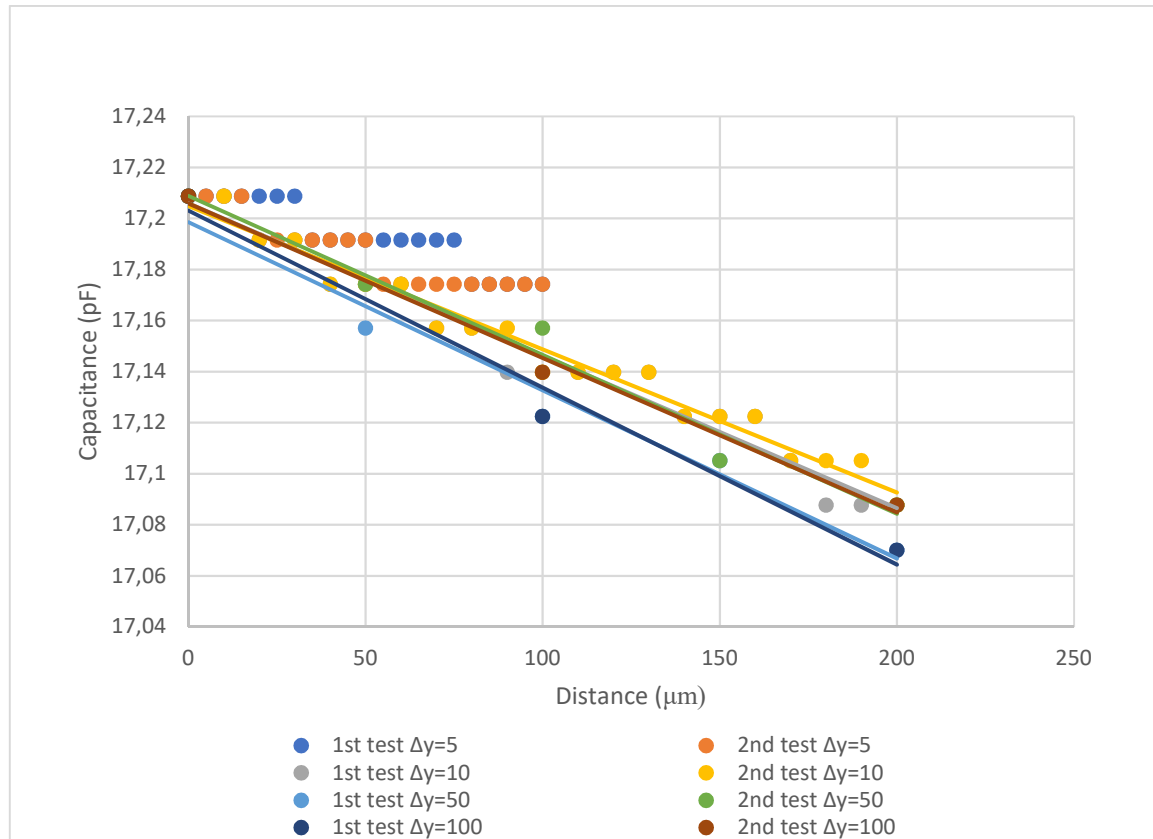


Figure 33: Adjusted results between 0 and 200 μm , for measured through phase shift, in a free of serum bone

For the experiments made with an interval of 5 μm , a decrease of 0.03 pF was seen for a distance of 100 μm . Because of the oscilloscope low resolution, only two shifts of capacitances were measured for this interval, hence a low correlation is seen when tracing a linear tendency line over these measurements. Therefore, only the experiments made with a larger interval were analysed in a linear manner. Table 8 shows the results obtained for these series of trials.

Δy [μm]	Test number	Tendency line equation	R^2
10	1 st test	$C = -0,0006d + 17,044$	0,9676
	2 nd test	$C = -0,0006d + 17,041$	0,9752
50	1 st test	$C = -0,0007d + 17,049$	0,9712
	2 nd test	$C = -0,0006d + 17,049$	0,9759
100	1 st test	$C = -0,0007d + 17,056$	0,9805
	2 nd test	$C = -0,0006d + 17,049$	0,9936

Table 8: Linear tendency line equation for the measured results, through phase shifts, for a bone free of serum

A mean variation of 0,63 fF for each micrometre is obtained.

4.2. Capacitance variations with saline solution

4.2.1. By measuring the resonant frequency

Like previous experiments, three experiments were conducted for each different interval. In Figure 34, and Table 9 the capacitive measurements with a bone, previously embedded in saline solution are showed, together with the quadratic tendency line equation for the intervals of 50 and 100 μm .

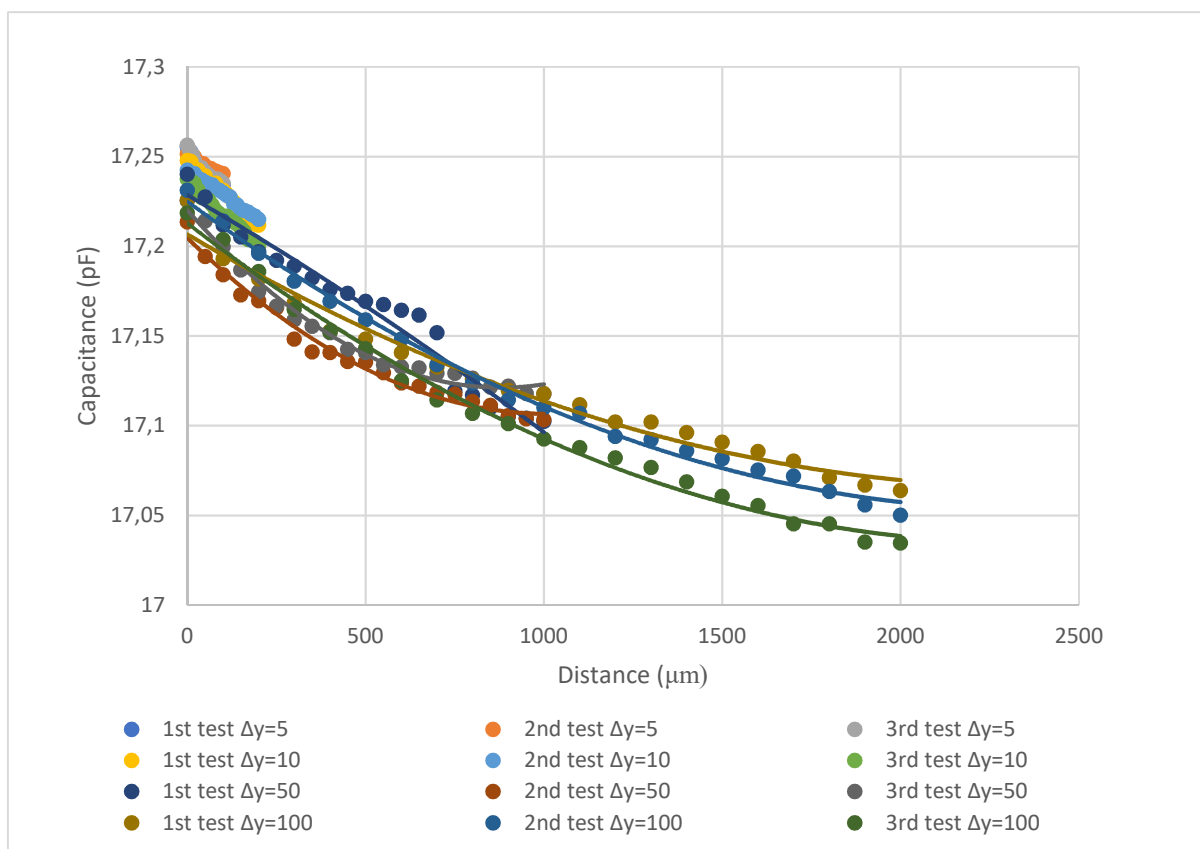


Figure 34: Results measured through resonant frequency measurement, for a bone previously embedded with saline solution

Δy [μm]	Test number	Tendency line equation	R^2
50	1 st test	$C = -2 \times 10^{-8} d^2 - 0,0001 d + 17,229$	0,9624
	2 nd test	$C = 1 \times 10^{-7} d^2 - 0,0002 d + 17,205$	0,984
	3 rd test	$C = 1 \times 10^{-7} d^2 - 0,0002 d + 17,220$	0,986
100	1 st test	$C = 2 \times 10^{-8} d^2 - 0,0001 d + 17,207$	0,9781
	2 nd test	$C = 3 \times 10^{-8} d^2 - 0,0001 d + 17,225$	0,9942
	3 rd test	$C = 3 \times 10^{-8} d^2 - 0,0002 d + 17,213$	0,9925

Table 9: Quadratic tendency line equation for the measured results, through resonant frequency measurement, for a bone previously embedded with saline solution

The first point measured varies from 17,219 pF to 17,256 pF. A high correlation is again obtained from tendency line equations. A decrease in the quadratic term is once again seen when a larger distance is measured.

A negative term is seen in the 1st test for a Δy equal to 50 μm . Observing these results between 700 and 800 μm , a sudden decrease in capacitance is observed. This occurred most likely due to the appearance of a saline solution drop in the interface of the bone. When the bone departs from the drop an abrupt change in the dielectric occurs, appearing a high decrease in capacitance. This phenomenon can be better seen in Figure 35, where these measurements were isolated.

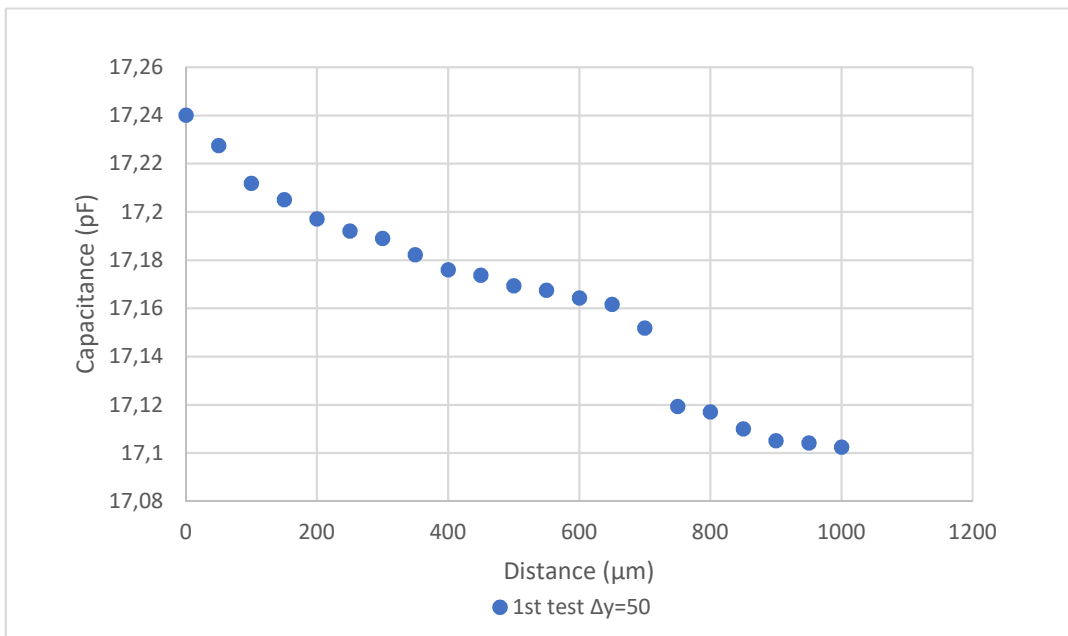


Figure 35: Results measured through resonant frequency measurement, for a bone previously embedded with saline solution with $\Delta y=50 \mu\text{m}$

Adjusting the measurement interval between 0 and 200 μm and tracing a linear tendency line, an approximation is showed in Figure 36 and Table 10.

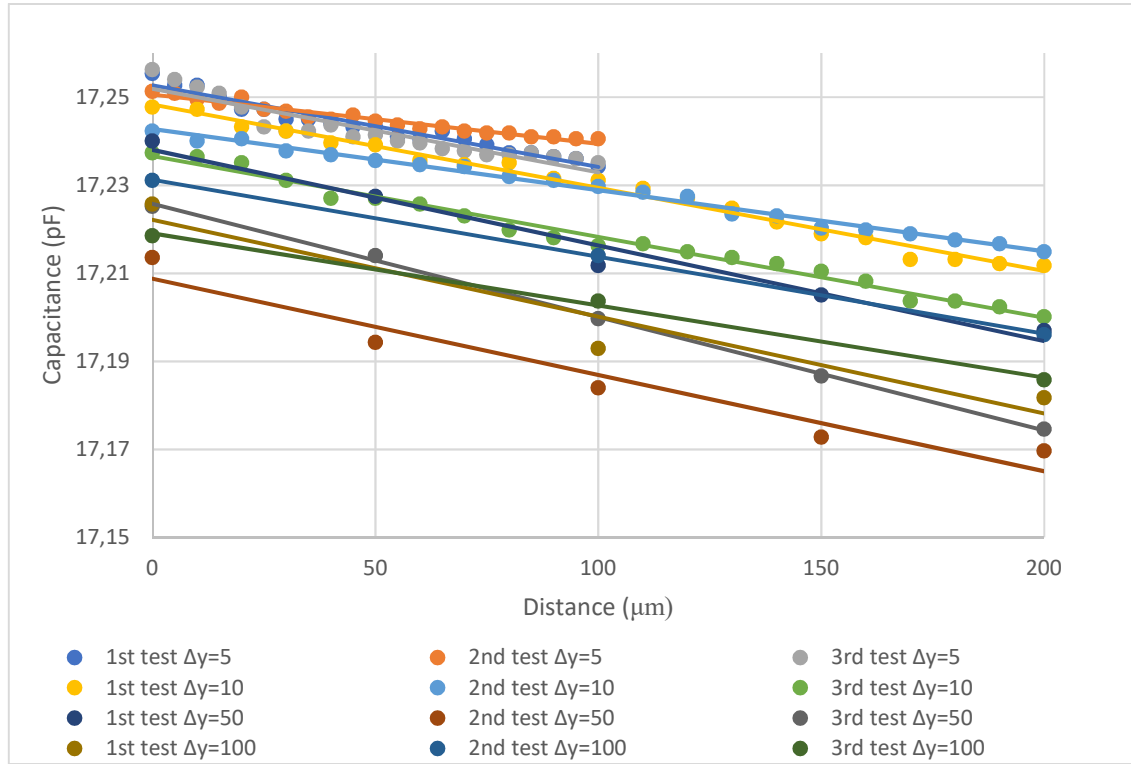


Figure 36: Adjusted results between 0 and 200 μm , through resonant frequency measurement, for a bone previously embedded in saline solution

Δy [μm]	Test number	Tendency line equation	R^2
5	1 st test	$C = -0,0002d + 17,253$	0,954
	2 nd test	$C = -0,0001d + 17,251$	0,9552
	3 rd test	$C = -0,0002d + 17,252$	0,8696
10	1 st test	$C = -0,0002d + 17,248$	0,9883
	2 nd test	$C = -0,0001d + 17,243$	0,9909
	3 rd test	$C = -0,0002d + 17,237$	0,9867
50	1 st test	$C = -0,0002d + 17,238$	0,9746
	2 nd test	$C = -0,0002d + 17,209$	0,9404
	3 rd test	$C = -0,0003d + 17,226$	0,9988
100	1 st test	$C = -0,0002d + 17,222$	0,9258
	2 nd test	$C = -0,0002d + 17,231$	0,9998
	3 rd test	$C = -0,0002d + 17,219$	0,997

Table 10: Linear tendency line equation for the measured results, through phase shifts, for a bone previously embedded saline solution

A decrease in capacitive variation is seen when comparing these results to the ones obtained with a bone free of serum. In this case a mean decrease of 0,19 fF is obtained per micrometer. Next results show the measurements obtained by analyzing the interface with phase changes.

4.2.2. By measuring phase shift

In the same manner as the previous evaluation, only 2 trials were made for each interval. The results are showed in Figure 37 and Table 11.

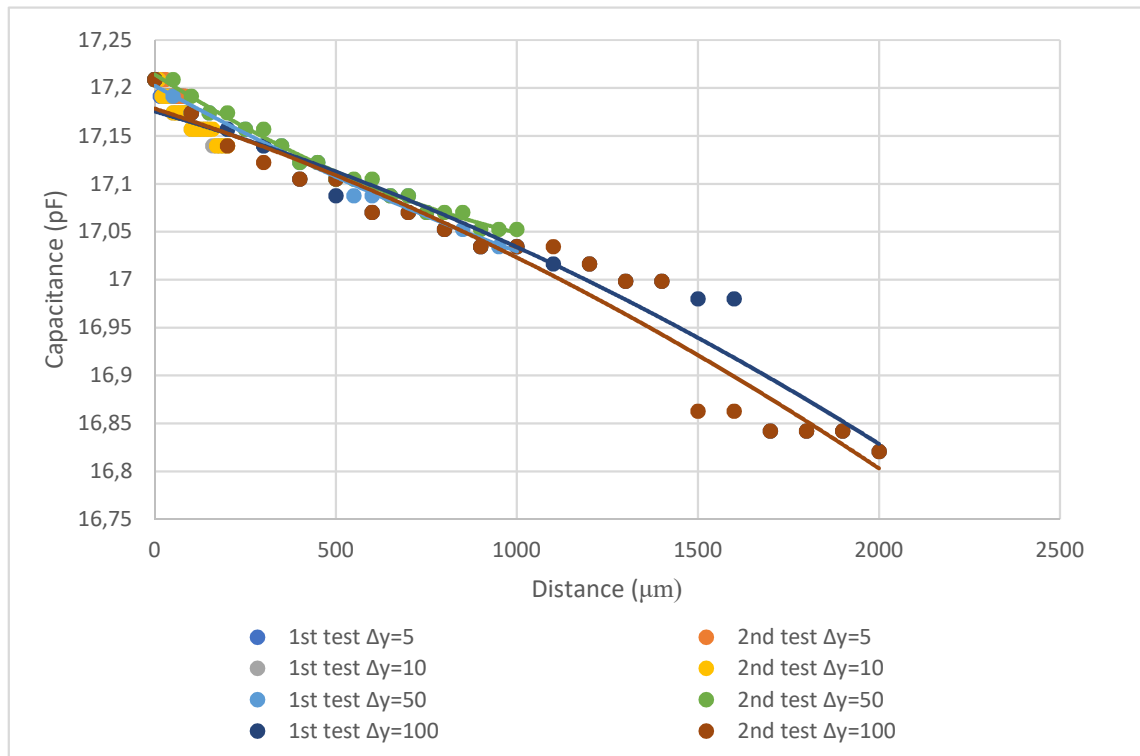


Figure 37: Results measured through phase shifts, for a bone previously embedded in saline solution

Δy [μm]	Test number	Tendency line equation	R^2
50	1 st attempt	$C = 3 \times 10^{-8} d^2 - 0,0002 d + 17,202$	0,987
	2 nd attempt	$C = 8 \times 10^{-8} d^2 - 0,0002 d + 17,213$	0,99
100	1 st attempt	$C = -3 \times 10^{-8} d^2 - 0,0001 d + 17,176$	0,9373
	2 nd attempt	$C = -3 \times 10^{-8} d^2 - 0,0001 d + 17,185$	0,9472

Table 11: Quadratic tendency line equation for the measured results, through phase shift measurement, for a bone previously embedded with saline solution

Again, a significant variation of measurements is seen, this time, between 1400 and 1700 μm . Again, this occur most likely due to the presence of a fluid drop beneath the bone surface. When the bone is pressed onto the structure, a mean capacitance of 17,205 pF is measured. Adjusting the graphic to an interval between 0 and 200 μm and tracing a linear tendency line over the results, the graphic of Figure 38, is obtained. Once again, only the measurements of 10, 50 and 100 μm were analysed in Table 12.

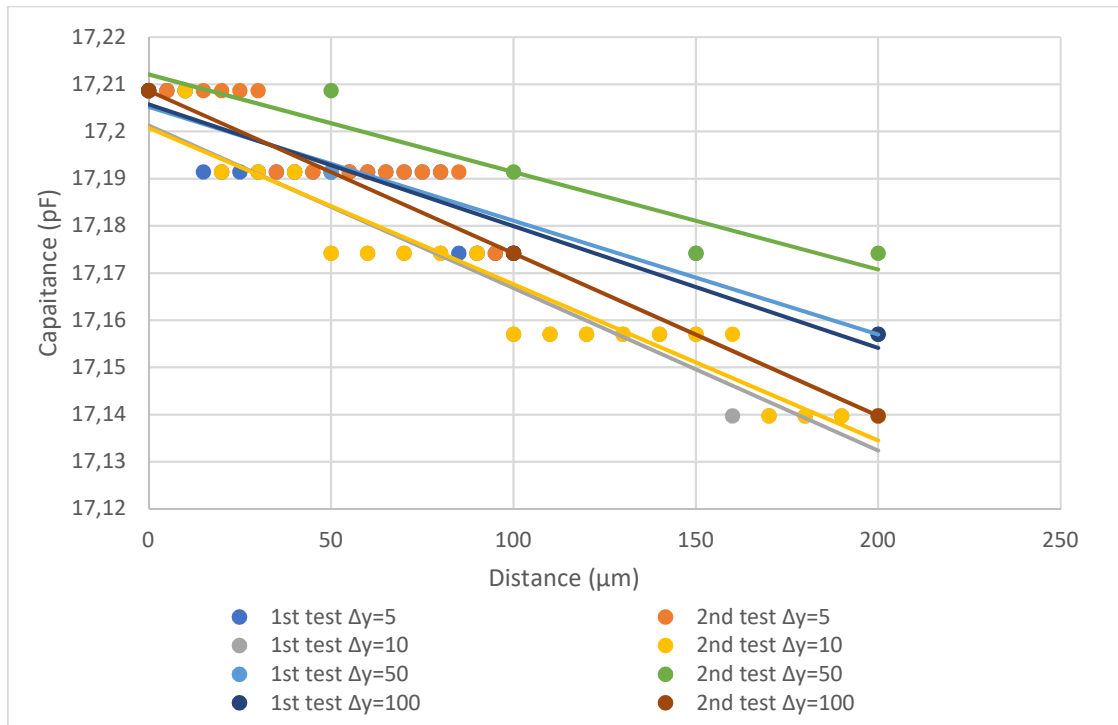


Figure 38: Adjusted results between 0 and 200 μm , through phase shift measurement, for a bone previously embedded in saline solution

Δy [μm]	Test number	Tendency line equation	R^2
10	1 st test	$C = -0,0003d + 17,208$	0,9294
	2 nd test	$C = -0,0003d + 17,203$	0,9191
50	1 st test	$C = -0,0002d + 17,204$	0,9423
	2 nd test	$C = -0,0002d + 17,211$	0,9
100	1 st test	$C = -0,0003d + 17,206$	0,9643
	2 nd test	$C = -0,0003d + 17,215$	1

Table 12: Linear tendency line equation for the measured results, through phase shifts, for a bone previously embedded saline solution

A significant decrease in the slope of the tendency line equations is obtained, when comparing to the results obtained using the same method for a bone without saline solution. An estimated decrease of 0,26 fF is obtained with these results. The mean decrease for each set of experiments, as well as the mean measurement for a “fixed implant” (first point measured), is described in Table 13.

Experiment	Measuring method	Mean slope (\bar{m}) [fF]	Mean capacitance for fixed prosthesis [pF]
Bone without saline solution	Voltage amplitude	0,23	17,143
	Phase differences	0,63	17,044
Bone with saline solution	Voltage amplitude	0,19	17,236
	Phase differences	0,26	17,205

Table 13: Global results for the experimental procedure.

5. Discussion

A decrease tendency of the capacitance with increasing distances between the cosurface capacitive system and the bone is clear in every set of measurements. It is also seen that, with the gradual increase of the distance between the bone and the cosurface capacitive system, the capacitance variation between measurement decreases, therefore a quadratic shape of the series of measurements is observed. Comparing the results obtained with the two measuring methods used, although it is seen a disagreement between the values obtained, the same pattern is obtained. These different results are mainly because of the poor resolution of the oscilloscope in measuring phase differences.

It was also observed different capacitances for a fixed implant, when comparing the values obtained with and without the saline solution. This is due to the higher relative permittivity of the water which decreases the resonant frequency and consequently increases the capacitance measured in the bone. The effect of embedding the bone previously in the saline solution is also noticed when comparing the mean slope between experiments. Due to the higher capacitance of the system, shorter capacitance variations are expected, which in turn are harder to detect. The impact of the fluid will most likely be more significant when using blood, since its relative permittivity has a higher value than the saline solution [124]. Besides, due to the high conductivity of the fluid, the magnetic waves

emitted from the electrodes can be lead away from the bone, thus influencing further the measured signal. The fluid in these measurements can be a crucial issue in future works.

Several difficulties occurred during the execution of these experiments. It is important to refer the low resolution obtained using an oscilloscope. Besides, the measurements were made, with changeable environment conditions, namely with temperature and relative humidity differences.

Repeatability of experiments is hard to evaluate. As different parts (of the same bone) were used, different topological structures were used as bone-implant interfaces. This last effect is more perceptible for the smaller intervals such as 5 and 10 μm , where capacitance increases in some regions in the interface occur as the gap between the cosurface capacitive system and the bone increases.

As a result of parasitic capacitances, only small changes are seen when elevating the bone from the measuring structure. When dealing with high accurate sensors, parasitic capacitances must be reduced as much as possible. In this case the influence of the stray capacitances comes mainly from the strips leading to the electrodes where the distance between lanes is reduced. A possible solution to this problem is to design a more sophisticated resonant circuit with low resonant frequencies. Besides, to avoid the influence of parasitic capacitances, computer-based signal analyses are easier to accomplished.

Another difficulty in this measurement method is to assure that the bone surface is completely in contact with the measurement surface of the structure, as well to ensure a non-contact condition to simulate loosen states. The bone was carefully prepared so than the bottom portion of the bone was parallel to the impact surface, and although a 2N force was provided, some portion of the bone may be in contact and providing pression, while in others a gap may be present. In future experiments, the setup needs to be redone, so that the bottom surface of the bone can be carefully analysed throughout experiments

6. Conclusions and future work

This work represents the starting point in a promising and pioneering methodology for sensing the interface between bone and implant, and from this work, several other studies could be pursued. It is conclusive that these method is an improvement in respect to X-rays, since with this setup differences of 5 μm were detectable. Also, its fulfils most conditions that an instrumented active implant must include:

- It operates as a therapeutic actuator.
- The electrodes small size assures an easy integration and flexibility inside the implants.

- This method assures a controllable monitoring, also, with the right disposition of electrodes various target regions of the tissues can be inspected.
- Although the developed setup is not able to identify the origin of the loosening effect, by connecting separately each pair of electrodes this problem can be overcome.
- It is still possible to conclude that this method operates in a non-invasively way, and with minimum interaction in the implant-bone interface.
- Distances of 5 μm were detectable, which suggests that this method is capable of monitoring the interface between bone and implant before severe loosening occurs.

Hence, capacitive monitoring is a methodology that must be explored in the future, and a viable alternative to current loosening monitoring devices.

Further research must be conducted to analyse the potential of using cosurface capacitive systems to monitor osseointegration. Most likely, the following works will be carried out in the forthcoming years:

- Different arrangements of electrodes should be studied. The impact of altering the plates area, and gap between each electrode should be studied and quantified.
- Parasitic capacitances could be further reduced in the present work. By reducing these unwanted capacitances, higher alterations of capacitance per micrometre should be detected. A way of achieving these results could be accomplished by significantly reducing the resonant frequency of the resonant circuit.
- The experimental apparatus must be redesigned. As previously mentioned, the bottom surface of the bone should be at all time monitored during experiments. This problem could be solved for instances, by placing a camera beneath the acrylic structure. Also, the device used to acquire the output voltage must be able to detect the resonant frequency in a precise manner.
- Development of FEM models to predict capacitance variations to different bone-implant interfaces. This will allow to accurately design a sophisticated resonant circuit.

7. Bibliography

- [1] A. J. Guyer and G. Richardson, "Current concepts review: total ankle arthroplasty.," *Foot ankle Int.*, vol. 29, no. 2, pp. 256–64, 2008.
- [2] S. Kurtz, K. Ong, E. Lau, F. Mowat, and M. Halpern, "Projections of primary and revision

- hip and knee arthroplasty in the United States from 2005 to 2030.," *J. Bone Joint Surg. Am.*, vol. 89, pp. 780–785, 2007.
- [3] S. M. Kurtz *et al.*, "International survey of primary and revision total knee replacement," *Int. Orthop.*, vol. 35, no. 12, pp. 1783–1789, 2011.
- [4] D. R. Sumner, "Long-term implant fixation and stress-shielding in total hip replacement," *J. Biomech.*, vol. 48, no. 5, pp. 797–800, 2015.
- [5] P. Mj and G. Ks, "Arthroplasties (with and without bone cement) for proximal femoral fractures in adults (Review)," *The Cochrane Library*, no. 2. 2006.
- [6] S. M. J. Mortazavi, J. Schwartzenger, M. S. Austin, J. J. Purtill, and J. Parvizi, "Revision total knee arthroplasty infection: incidence and predictors.," *Clin. Orthop. Relat. Res.*, vol. 468, no. 8, pp. 2052–2059, 2010.
- [7] S. M. Jafari, C. Coyle, S. M. J. Mortazavi, P. F. Sharkey, and J. Parvizi, "Revision hip arthroplasty: Infection is the most common cause of failure," *Clin. Orthop. Relat. Res.*, vol. 468, no. 8, pp. 2046–2051, 2010.
- [8] G. Labek, M. Thaler, W. Janda, M. Agreiter, and B. Stöckl, "Revision rates after total joint replacement," *J Bone Jt. Surg [Br]*, vol. 93, no. 3, pp. 293–7, 2011.
- [9] K. J. SALEH, J. A. RAND, and D. A. MCQUEEN, "Current Status of Revision Total Knee Arthroplasty," *J. Bone Jt. Surgery-American Vol.*, vol. 85, no. February 2003, pp. 18–20, 2003.
- [10] N. authors listed, "American Joint Replacement Registry," 2016. [Online]. Available: <http://www.ajrr.net>.
- [11] M. P. Soares, A. Marote, T. Santos, J. Torrão, and A. Ramos, "New cosurface capacitive stimulators for the development of active osseointegrative implantable devices," *Nat. Publ. Gr.*, no. February, pp. 1–15, 2016.
- [12] D. Aletaha *et al.*, "2010 Rheumatoid arthritis classification criteria: An American College of Rheumatology/European League Against Rheumatism collaborative initiative," *Arthritis Rheum.*, vol. 62, no. 9, pp. 2569–2581, 2010.
- [13] S. Gabriele, "The epidemiology of rheumatoid arthritis," *Arthritis Rheum.*, vol. 8, no. 1, pp. 76–79, 1965.
- [14] J. S. Smolen, D. Aletaha, M. Koeller, M. H. Weisman, and P. Emery, "New therapies for treatment of rheumatoid arthritis," *Lancet*, vol. 370, no. 9602, pp. 1861–1874, 2007.
- [15] G. S. Firestein, "Evolving concepts of rheumatoid arthritis.," *Nature*, vol. 423, no. 6937, pp. 356–61, 2003.
- [16] N. authors Listed, "National Joint Registry." [Online]. Available: <http://www.njrcentre.org.uk>.

- [17] D. T. Felson, R. Lawrence, P. Dieppe, and R. Hirsch, "NIH Conference Osteoarthritis : New Insights," *Ann. Intern. Med.*, vol. 133, no. 8, pp. 637–639, 2000.
- [18] R. Altman *et al.*, "The American College of Rheumatology criteria for the classification and reporting of osteoarthritis of the hip," *Arthritis Rheum.*, vol. 34, no. 5, pp. 505–514, 1991.
- [19] J. L. van Saase, L. K. van Romunde, A. Cats, J. P. Vandenbroucke, and H. A. Valkenburg, "Epidemiology of osteoarthritis: Zoetermeer survey. Comparison of radiological osteoarthritis in a Dutch population with that in 10 other populations.," *Ann. Rheum. Dis.*, vol. 48, no. 4, pp. 271–80, 1989.
- [20] J. Guerra and M. Steinberg, "Current Concepts Review Distinguishing Transient Osteoporosis from Avascular Necrosis of the Hip," *J. Bone Jt. Surg.*, pp. 616–624, 1995.
- [21] M. Mont and D. Hungerford, "Current Concepts Review: Non-Traumatic Avascular Necrosis of the Femoral Head," *J. Bone Jt. Surg.*, vol. 77, no. 3, pp. 616–624, 1995.
- [22] N. authors Listed, "Australian Orthopaedic Association, National Joint Replacement Registry." Hip, Knee & Shoulder Arthroplasty Annual Report, pp. 19–70, 2016.
- [23] N. Author, "Nasjonalt Register for Leddproteser," 2007. [Online]. Available: <http://nrlweb.ihelse.net/eng/>.
- [24] T. Dixon, "Trends in hip and knee joint replacement: socioeconomic inequalities and projections of need," *Ann. Rheum. Dis.*, vol. 63, no. 7, pp. 825–830, 2004.
- [25] S. M. Kurtz, E. Lau, K. Ong, K. Zhao, M. Kelly, and K. J. Bozic, "Future young patient demand for primary and revision joint replacement: National projections from 2010 to 2030," *Clin. Orthop. Relat. Res.*, vol. 467, no. 10, pp. 2606–2612, 2009.
- [26] D. Culliford, J. Maskell, A. Judge, C. Cooper, D. Prieto-Alhambra, and N. K. Arden, "Future projections of total hip and knee arthroplasty in the UK: Results from the UK Clinical Practice Research Datalink," *Osteoarthr. Cartil.*, vol. 23, no. 4, pp. 594–600, 2015.
- [27] A. Del Buono, V. Denaro, and N. Maffulli, "Genetic susceptibility to aseptic loosening following total hip arthroplasty: A systematic review," *Br. Med. Bull.*, vol. 101, no. 1, pp. 39–55, 2012.
- [28] F. Birrell, O. Johnell, and A. Silman, "Projecting the need for hip replacement over the next three decades: influence of changing demography and threshold for surgery.," *Ann. Rheum. Dis.*, vol. 58, no. 9, pp. 569–72, 1999.
- [29] A. Rothwell, A. Oakley, P. Larmer, T. Hobbs, and A. Rothwell, "THE NEW ZEALAND Annual Report Editorial Committee," no. January 1999, 2015.
- [30] N. authors listed, "Population of New Zealand 2015 - PopulationPyramid." [Online]. Available: <http://www.populationpyramid.net/new-zealand/2015/>.
- [31] S. H. Kim, B. L. Wise, Y. Zhang, and R. M. Szabo, "Increasing incidence of shoulder

- arthroplasty in the United States,” *J. Bone Jt. Surg. - Ser. A*, vol. 93, no. 24, pp. 2249–2254, 2011.
- [32] J. S. Day, E. Lau, K. L. Ong, G. R. Williams, M. L. Ramsey, and S. M. Kurtz, “Prevalence and projections of total shoulder and elbow arthroplasty in the United States to 2015,” *Journal of Shoulder and Elbow Surgery*, vol. 19, no. 8, pp. 1115–1120, 2010.
- [33] C. Wainwright, J.-C. Theis, N. Garneti, and M. Melloh, “Age at hip or knee joint replacement surgery predicts likelihood of revision surgery,” *J. Bone Joint Surg. Br.*, vol. 93, no. 10, pp. 1411–5, 2011.
- [34] J. D. Dieterich, A. C. Fields, and C. S. Moucha, “Short term outcomes of revision total knee arthroplasty,” *J. Arthroplasty*, vol. 29, no. 11, pp. 2163–6, 2014.
- [35] K. J. Mulhall, H. M. Ghomrawi, S. Scully, J. J. Callaghan, and K. J. Saleh, “Current etiologies and modes of failure in total knee arthroplasty revision,” *Clin. Orthop. Relat. Res.*, vol. 446, no. 446, pp. 45–50, 2006.
- [36] C. Lavernia, D. J. Lee, and V. H. Hernandez, “The increasing financial burden of knee revision surgery in the United States,” *Clin. Orthop. Relat. Res.*, vol. 446, no. 446, pp. 221–6, 2006.
- [37] N. authors Listed, “SPOT. Registo Português de Artroplastias,” 2016. [Online]. Available: <http://www.rpa.spot.pt>.
- [38] M. T. Dillon *et al.*, “The Kaiser Permanente shoulder arthroplasty registry: results from 6,336 primary shoulder arthroplasties,” *Acta Orthop*, vol. 86, no. 3, pp. 286–292, 2015.
- [39] F. F. Buechel and M. J. Pappas, *Principles of Human Joint Replacement*, no. July. 2015.
- [40] D. Van Harlingen, P. J. Heesterbeek, and M. Vos, “High rate of complications and radiographic loosening of the biaxial total wrist arthroplasty in rheumatoid arthritis,” *Acta Orthop.*, vol. 82, no. 6, pp. 721–726, 2011.
- [41] P. Boileau, R. J. Sinnerton, C. Chuinard, and G. Walch, “Review Article: Arthroplasty of the shoulder,” *J. Bone Jt. Surgery-American Vol.*, vol. 51, no. 4, pp. 562–575, 2006.
- [42] Y. Abu-Amer, I. Darwech, and J. C. Clohisy, “Aseptic loosening of total joint replacements: mechanisms underlying osteolysis and potential therapies,” *Arthritis Res. Ther.*, vol. 9 Suppl 1, p. S6, 2007.
- [43] A. Completo and F. Fonseca, *Fundamentos de Biomecânica: Músculo-Esquelética e Ortopédica*, 2^a. 2011.
- [44] E. F. Eriksen, H. J. G. Gundersen, F. Melsen, and L. Mosekilde, “Reconstruction of the formative site in iliac trabecular bone in 20 normal individuals employing a kinetic model for matrix and mineral apposition,” *Metab. Bone Dis. Relat. Res.*, vol. 5, no. 5, pp. 243–252, 1984.

- [45] B. G. U. Exner, A. Prader, U. Elsasser, P. Rueggsegger, and M. Anliker, "Bone densitometry using computed tomography," no. Part II, pp. 14–23, 1979.
- [46] A. S. Carlsson, C.-F. Gentz, and L. Linder, "Localized bone resorption in the femur in mechanical failure of cemented total hip arthroplasties," *Acta Orthop. Scand.*, vol. 54, no. 3, pp. 396–402, 1983.
- [47] P. A. Banaszkiwicz and D. F. Kader, *Classic papers in orthopaedics*. 2014.
- [48] P. Doorn, P. Campbell, J. Worrall, P. Benya, H. McKellop, and H. Amstutz, "Metal wear particle characterization from metal on metal total hip replacements: Transmission electron microscopy study of periprosthetic tissue and isolate particles," *John Wiley Sons, Inc*, vol. 4636, no. November 1998, 1998.
- [49] M. Sundfeldt, L. V Carlsson, C. B Johansson, P. Thomsen, and C. Gretzer, "Aseptic loosening, not only a question of wear: A review of different theories," *Acta Orthop.*, vol. 77, no. 2, pp. 177–197, 2006.
- [50] G. Lewis, "Properties of acrylic bone cement: state of the art review.," *J. Biomed. Mater. Res.*, vol. 38, no. February, pp. 155–82, 1997.
- [51] P. A. Banaszkiwicz, "Reactions of the articular capsule to wear products of artificial joint prostheses," *Class. Pap. Orthop.*, vol. 11, pp. 77–79, 2014.
- [52] H. Warashina *et al.*, "Biological reaction to alumina, zirconia, titanium and polyethylene particles implanted onto murine calvaria," *Biomaterials*, vol. 24, no. 21, pp. 3655–3661, 2003.
- [53] a Hatton, J. E. Nevelos, J. B. Matthews, J. Fisher, and E. Ingham, "Effects of clinically relevant alumina ceramic wear particles on TNF-alpha production by human peripheral blood mononuclear phagocytes.," *Biomaterials*, vol. 24, no. 7, pp. 1193–204, 2003.
- [54] J. Nagels, M. Stokdijk, and P. M. Rozing, "Stress shielding and bone resorption in shoulder arthroplasty," *J. Shoulder Elb. Surg.*, vol. 12, no. 1, pp. 35–39, 2003.
- [55] M. G. Joshi, S. G. Advani, F. Miller, and M. H. Santare, "Analysis of a femoral hip prosthesis designed to reduce stress shielding," *J. Biomech.*, vol. 33, no. 12, pp. 1655–1662, 2000.
- [56] M. Varga and K.-J. Wolter, "Sensors and imaging methods for detecting loosening of orthopedic implants - a review," *IEEE 20th Int. Symp. Des. Technol. Electron. Packag.*, pp. 333–335, 2014.
- [57] C. Ruther, U. Timm, H. Ewal, W. Mittelmeier, R. Bader, and R. Schmelter, "Current possibilities for detection of loosening of total hip replacements and how intelligent implants could improve diagnostic accuracy," *Recent Adv. Arthroplast.*, no. March 2017, pp. 363–386, 2012.

- [58] J. Andreu Perez, D. Leff, H. Ip, and G.-Z. Yang, "From Wearable Sensors to Smart Implants - Towards Pervasive and Personalised Healthcare.," *IEEE Trans. Biomed. Eng.*, vol. 62, no. 12, pp. 2750–2762, 2015.
- [59] M. Atsumi, S. Park, and H. Wang, "Methods used to assess implant stability: current status.," *Oral Maxillofac. Implant.*, 2007.
- [60] J.-C. Park, J.-W. Lee, S.-M. Kim, and J.-H. Lee, "Implant Stability - Measuring Devices and Randomized Clinical Trial for ISQ Value Change Pattern Measured from Two Different Directions by Magnetic RFA," *Implant Dent. - A Rapidly Evol. Pract.*, no. Meredith 1998, 2011.
- [61] A. Sachdeva, P. Dhawan, S. Sindwani, and I. M. El-Sayed El-Hakim, "Assessment of Implant Stability: Methods and Recent Advances," *Br. J. Med. Med. Res. Crit. Care Trauma Hosp. India. Sachdeva al*, vol. 12, no. 123, pp. 1–10, 2016.
- [62] Y. Zhang, A. W. Putnam, A. D. Heiner, J. J. Callaghan, and T. D. Brown, "Reliability of detecting prosthesis/cement interface radiolucencies in total hip arthroplasty," *J. Orthop. Res.*, vol. 20, no. 4, pp. 683–687, 2002.
- [63] C. Phillip and S. Kattapuram, "Prosthetic Hip Replacements : Plain Films and Arthrography for Component Loosening," *Dep. Radiol. Massachusetts Gen. Hosp. Harvard Med. Sch. Bost.*, pp. 677–682, 1981.
- [64] D. M. Mulcahy, G. C. C. Fenelon, and D. P. McInerney, "Aspiration Arthrography of the Hip Joint Its Uses and Limitations in Revision Hip Surgery," *J. Arthroplast.*, vol. 11, no. 1, pp. 64–68, 1996.
- [65] T. H. French, N. Russell, and A. Pillai, "The diagnostic accuracy of radionuclide arthrography for prosthetic loosening in hip and knee arthroplasty," *Biomed Res. Int.*, vol. 2013, no. April 2010, 2013.
- [66] J. T. Abele, V. G. Swami, G. Russell, E. C. O. Masson, and J. P. Flemming, "The Accuracy of Single Photon Emission Computed Tomography/Computed Tomography Arthrography in Evaluating Aseptic Loosening of Hip and Knee Prostheses," *J. Arthroplasty*, vol. 30, no. 9, pp. 1647–1651, 2015.
- [67] C. G. Chew, P. Lewis, F. Middleton, R. Van Den Wijngaard, and A. Deshaies, "Radionuclide arthrogram with SPECT/CT for the evaluation of mechanical loosening of hip and knee prostheses," *Ann. Nucl. Med.*, vol. 24, no. 10, pp. 735–743, 2010.
- [68] A. Rowlands, F. A. Duck, and J. L. Cunningham, "Bone vibration measurement using ultrasound: Application to detection of hip prosthesis loosening," *Med. Eng. Phys.*, vol. 30, no. 3, pp. 278–284, 2008.
- [69] L. Claassen, M. Ettinger, C. Plaass, K. Daniilidis, T. Calliess, and M. Ezechieli, "Diagnostic

- value of bone scintigraphy for aseptic loosening after total knee arthroplasty,” *Technol. Heal. Care*, vol. 22, no. 5, pp. 767–773, 2014.
- [70] M. P. Soares dos Santos *et al.*, “Instrumented hip joint replacements, femoral replacements and femoral fracture stabilizers,” *Expert Rev. Med. Devices*, vol. 11, no. 6, pp. 617–635, 2014.
- [71] N. W. Rydell, “Forces Acting on the Femoral Head-Prosthesis: A Study on Strain Gauge Supplied Prostheses in Living Persons,” *Acta Orthop. Scand.*, vol. 37, no. sup88, pp. 1–132, 1966.
- [72] D. A. Sonstegard and L. S. Matthews, “Sonic Diagnosis of Bone Fracture Preliminary Study,” vol. 9, no. May, pp. 689–694, 1976.
- [73] G. Van Der Perre and G. Lowet, “In vivo assessment of bone mechanical properties by vibration and ultrasonic wave propagation analysis,” *Bone*, vol. 18, no. 1 Suppl, p. 29S–35S, 1996.
- [74] A. D. Rosenstein, G. F. McCoy, C. J. Bulstrode, P. D. McLardy-Smith, J. L. Cunningham, and a R. Turner-Smith, “The differentiation of loose and secure femoral implants in total hip replacement using a vibrational technique: an anatomical and pilot clinical study,” *Proc. Inst. Mech. Eng. H.*, vol. 203, no. 2, pp. 77–81, 1989.
- [75] N. Meredith, F. Shagaldi, D. Alleyne, L. Sennerby, and P. Cawley, “The application of resonance frequency measurements to study the stability of titanium implants during healing in the rabbit tibia.pdf,” *Clin. Oral Implants Res.*, vol. 8, pp. 234–243, 1997.
- [76] P. Li, N. Jones, and P. Gregg, “Vibration prosthetic analysis in the detection loosening of total hip,” *October*, 1996.
- [77] A. P. Georgiou and J. L. Cunningham, “Accurate diagnosis of hip prosthesis loosening using a vibrational technique,” *Clin. Biomech.*, vol. 16, no. 4, pp. 315–323, 2001.
- [78] G. Qi, W. P. Mouchon, and T. E. Tan, “How much can a vibrational diagnostic tool reveal in total hip arthroplasty loosening?,” *Clin. Biomech.*, vol. 18, no. 5, pp. 444–458, 2003.
- [79] A. A. Alshuhri, T. P. Holsgrove, A. W. Miles, and J. L. Cunningham, “Development of a non-invasive diagnostic technique for acetabular component loosening in total hip replacements,” *Med. Eng. Phys.*, vol. 37, no. 8, pp. 739–745, 2015.
- [80] M. C. Dahl, P. A. Kramer, P. G. Reinhall, S. K. Benirschke, S. T. Hansen, and R. P. Ching, “The efficacy of using vibrometry to detect osteointegration of the Agility total ankle,” *J. Biomech.*, vol. 43, no. 9, pp. 1840–1843, 2010.
- [81] J. S. Rieger, S. Jaeger, C. Schuld, J. P. Kretzer, and R. G. Bitsch, “A vibrational technique for diagnosing loosened total hip endoprostheses: An experimental sawbone study,” *Med. Eng. Phys.*, vol. 35, no. 3, pp. 329–337, 2013.

- [82] R. Puers *et al.*, “Telemetry system for the detection of hip prosthesis loosening by vibration analysis,” *Sensors Actuators, A Phys.*, vol. 85, no. 1, pp. 42–47, 2000.
- [83] U. Marschner *et al.*, “Integration of a wireless lock-in measurement of hip prosthesis vibrations for loosening detection,” *Sensors Actuators, A Phys.*, vol. 156, no. 1, pp. 145–154, 2009.
- [84] S. Sauer and U. Marschner, “Medical wireless vibration measurement system for hip prosthesis loosening detection,” ... *2012, Third ...*, no. c, pp. 9–13, 2012.
- [85] J. S. Rieger, S. Jaeger, J. P. Kretzer, R. Rupp, and R. G. Bitsch, “Loosening detection of the femoral component of hip prostheses with extracorporeal shockwaves: A pilot study,” *Med. Eng. Phys.*, vol. 37, no. 2, pp. 157–164, 2015.
- [86] C. Scruby, “An introduction to acoustic emission,” *J. Phys. E.*, vol. 20, no. 8, pp. 946–953, 1987.
- [87] S. Shrivastava, “Assessment of bone condition by acoustic emission technique,” *J. Biomed. Sci. Eng.*, vol. 2, no. 3, pp. 144–154, 2009.
- [88] J. P. Davies, M.-K. Tse, and W. H. Harris, “Monitoring the integrity of the cement—metal interface of total joint components in vitro using acoustic emission and ultrasound,” *J. Arthroplasty*, vol. 11, no. 5, pp. 594–601, 1996.
- [89] J. P. Davies, M. -K Tse, and W. H. Harris, “In vitro evaluation of bonding of the cement-metal interface of a total hip femoral component using ultrasound,” *J. Orthop. Res.*, vol. 13, no. 3, pp. 335–338, 1995.
- [90] A. C. Unger, H. Cabrera-Palacios, A. P. Schulz, C. Jürgens, and A. Paech, “Acoustic monitoring (RFM) of total hip arthroplasty Results of a cadaver study,” *Eur. J. Med. Res.*, pp. 264–271, 2009.
- [91] A. Paech, H. Cabrera-Palacios, and A. P. Schulz, “Acoustic Tests on hip Prosthesis models using frequency resonance monitoring.pdf,” *Res. J. Meical Sci.*, 2008.
- [92] A. Roques, M. Browne, J. Thompson, C. Rowland, and A. Taylor, “Investigation of fatigue crack growth in acrylic bone cement using the acoustic emission technique,” *Biomaterials*, vol. 25, no. 5, pp. 769–778, 2004.
- [93] M. Mavrogordato, M. Taylor, A. Taylor, and M. Browne, “Real time monitoring of progressive damage during loading of a simplified total hip stem construct using embedded acoustic emission sensors,” *Med. Eng. Phys.*, vol. 33, no. 4, pp. 395–406, 2011.
- [94] H. Ewald, U. Timm, C. Ruther, W. Mittelmeier, R. Bader, and D. Kluess, “Acoustic sensor system for loosening detection of hip implants,” *Proc. Int. Conf. Sens. Technol. ICST*, pp. 494–497, 2011.
- [95] A. J. Fitzpatrick, G. W. Rodgers, G. J. Hooper, and T. B. F. Woodfield, “Development and

- validation of an acoustic emission device to measure wear in total hip replacements in-vitro and in-vivo,” *Biomed. Signal Process. Control*, vol. 33, pp. 281–288, 2017.
- [96] G. W. Rodgers, R. Welsh, L. J. King, A. FitzPatrick, T. B. F. Woodfield, and G. J. Hooper, “Signal processing and event detection of hip implant acoustic emissions,” *Control Eng. Pract.*, vol. 58, no. May 2016, pp. 287–297, 2015.
- [97] C. L. Brockett, S. Williams, Z. Jin, G. H. Isaac, and J. Fisher, “Squeaking Hip Arthroplasties: A Tribological Phenomenon,” *J. Arthroplasty*, vol. 28, no. 1, pp. 90–97, 2013.
- [98] C. Chevillotte, V. Pibarot, J. P. Carret, J. Bejui-Hugues, and O. Guyen, “Hip Squeaking. A 10-Year Follow-Up Study,” *J. Arthroplasty*, vol. 27, no. 6, pp. 1008–1013, 2012.
- [99] C. Chevillotte, R. T. Trousdale, K. N. An, D. Padgett, and T. Wright, “Retrieval analysis of squeaking ceramic implants: Are there related specific features?,” *Orthop. Traumatol. Surg. Res.*, vol. 98, no. 3, pp. 281–287, 2012.
- [100] C. Ruther, H. Ewald, W. Mittelmeier, A. Fritsche, R. Bader, and D. Klues, “A Novel Sensor Concept for Optimization of Loosening Diagnostics in Total Hip Replacement,” *J. Biomech. Eng.*, vol. 133, no. 10, p. 104503, 2011.
- [101] C. Ruther *et al.*, “Investigation of a passive sensor array for diagnosis of loosening of endoprosthetic implants,” *Sensors (Basel)*, vol. 13, no. 1, pp. 1–20, 2012.
- [102] C. Ruther *et al.*, “Investigation of an acoustic-mechanical method to detect implant loosening,” *Med. Eng. Phys.*, vol. 35, no. 11, pp. 1669–1675, 2013.
- [103] C. Ruther *et al.*, “In vivo monitoring of implant osseointegration in a rabbit model using acoustic sound analysis,” *J. Orthop. Res.*, vol. 32, no. 4, pp. 606–612, 2014.
- [104] J.-P. Morucci, M. E. Valentinuzzi, B. Rigaud, C. J. Felice, N. Chauveau, and P.-M. Marsili, “Bioelectric Impedance Techniques in Medicine,” *Critical Reviews in Biomedical Engineering*, vol. 24, no. 4–6, pp. 257–338, 1996.
- [105] J. L. Mueller, S. Siltanen, and D. Isaacson, “A direct reconstruction algorithm for electrical impedance tomography,” *Med. Imaging, IEEE Trans.*, vol. 21, no. 6, pp. 555–559, 2002.
- [106] P. Arpaia, F. Clemente, and A. Zanesco, “Low-invasive diagnosis of metallic prosthesis osseointegration by electrical impedance spectroscopy,” *IEEE Trans. Instrum. Meas.*, vol. 56, no. 3, pp. 784–789, 2007.
- [107] P. Arpaia, F. Clemente, and C. Romanucci, “In-vivo test procedure and instrument characterization for EIS-based diagnosis of prosthesis osseointegration,” *Conf. Rec. - IEEE Instrum. Meas. Technol. Conf.*, pp. 1–6, 2007.
- [108] P. Arpaia, P. Cimmino, F. Clemente, and C. Romanucci, “A microcontroller-based instrument for prostheses osseointegration measurement by electrochemical impedance

- spectroscopy,” *Measurements*, vol. 41, no. 9, pp. 1040–1044, 2007.
- [109] J. Kärrholm, B. Borssén, G. Löwenhielm, and F. Snorrason, “Does early micromotion of femoral stem prostheses matter? 4-7-year stereoradiographic follow-up of 84 cemented prostheses,” *J. Bone Joint Surg. Br.*, vol. 76, no. 6, pp. 912–7, 1994.
- [110] S. A. Maher and P. J. Prendergast, “Discriminating the loosening behaviour of cemented hip prostheses using measurements of migration and inducible displacement,” *J. Biomech.*, vol. 35, no. 2, pp. 257–265, 2002.
- [111] S. Hao, J. T. Taylor, C. R. Bowen, S. Gheduzzi, and A. W. Miles, “Sensing methodology for in vivo stability evaluation of total hip and knee arthroplasty,” *Sensors Actuators, A Phys.*, vol. 157, no. 1, pp. 150–160, 2010.
- [112] S. Hao, J. Taylor, A. W. Miles, and C. R. Bowen, “An implantable system for the in vivo measurement of hip and knee migration and micromotion,” *ICSES’08 - ICSES 2008 Int. Conf. Signals Electron. Syst. Proc.*, pp. 445–448, 2008.
- [113] T. Fresvig, P. Ludvigsen, H. Steen, and O. Reikerås, “Fibre optic Bragg grating sensors: An alternative method to strain gauges for measuring deformation in bone,” *Med. Eng. Phys.*, vol. 30, no. 1, pp. 104–108, 2008.
- [114] N. Lajnef, S. Chakrabartty, N. Elvin, and A. Elvin, “Piezo-powered floating gate injector for self-powered fatigue monitoring in biomechanical implants,” *Circuits Syst. 2007. ISCAS 2007. IEEE Int. Symp.*, pp. 89–92, 2007.
- [115] P. Alpuim *et al.*, “Fabrication of a strain sensor for bone implant failure detection based on piezoresistive doped nanocrystalline silicon,” *J. Non. Cryst. Solids*, vol. 354, no. 19–25, pp. 2585–2589, 2008.
- [116] K. C. McGilvray *et al.*, “Implantable microelectromechanical sensors for diagnostic monitoring and post-surgical prediction of bone fracture healing,” *J. Orthop. Res.*, vol. 33, no. 10, pp. 1439–1446, 2015.
- [117] K. Kroncke, K. Fehsel, and V. Kolb-Bachofen, “Inducible nitric oxide synthase in human diseases,” *Clin. Exp. Immunol.*, vol. 113, no. 2, pp. 147–156, 1998.
- [118] F. Yang *et al.*, “Pathways of macrophage apoptosis within the interface membrane in aseptic loosening of prostheses,” *Biomaterials*, vol. 32, no. 35, pp. 9159–9167, 2011.
- [119] S. Stea *et al.*, “Nitric oxide synthase in tissues around failed hip prostheses,” *Biomaterials*, vol. 23, no. 24, pp. 4833–4838, 2002.
- [120] M. J. Steinbeck, L. J. Jablonowski, J. Parvizi, and T. A. Freeman, “The Role of Oxidative Stress in Aseptic Loosening of Total Hip Arthroplasties,” *J. Arthroplasty*, vol. 29, no. 4, pp. 843–849, 2014.
- [121] D. Granchi *et al.*, “Serum levels of osteoprotegerin and receptor activator of nuclear factor-

- kappaB ligand as markers of periprosthetic osteolysis.," *J. Bone Joint Surg. Am.*, vol. 88, no. 7, pp. 1501–9, 2006.
- [122] S. Landgraeber *et al.*, "Tartrate-resistant acid phosphatase 5b and C-terminal telopeptides of type i collagen as markers for diagnosis of aseptic loosening after total hip replacement," *Arch. Orthop. Trauma Surg.*, vol. 130, no. 4, pp. 441–445, 2010.
- [123] A. Stogryn, "Equations for Calculating the Dielectric Constant of Saline Water," *IEEE Trans. Microw. Theory Tech.*, vol. 19, no. 8, pp. 733–736, 1971.
- [124] A. R. F Jaspard, M Nadi, "Dielectric properties of blood : an investigation of haematocrit dependence," *IOP J.*, vol. 137, pp. 138–147, 2003.